In vitro efficacy of a gene-activated nerve guidance conduit incorporating non-viral PEI-pDNA nanoparticles carrying genes encoding for NGF, GDNF and c-Jun.

AUTHOR(S)

William A. Lackington, Rosanne M. Raftery, Fergal J. O'Brien

Title

In vitro efficacy of a gene-activated nerve guidance conduit incorporating non-viral PEI-pDNA nanoparticles carrying genes encoding for NGF, GDNF and c-Jun

Authors

William A. Lackington[1,2,3], Rosanne M. Raftery[1,2,3] and Fergal J. O'Brien[1,2,3]

[1]Tissue Engineering Research Group (TERG), Department of Anatomy, Royal College of Surgeons in Ireland.
[2]Advanced Materials and Bioengineering Research (AMBER) Centre, Trinity College Dublin, Ireland.
[3]Trinity Centre for Bioengineering (TCBE), Trinity College Dublin, Ireland.

Abstract

Despite the success of tissue engineered nerve guidance conduits (NGCs) for the treatment of small peripheral nerve injuries, autografts remain the clinical gold standard for larger injuries. The delivery of neurotrophic factors from conduits might enhance repair for more effective treatment of larger injuries but the efficacy of such systems is dependent on a safe, effective platform for controlled and localised therapeutic delivery. Gene therapy might offer an innovative approach to control the timing, release and level of neurotrophic factor production by directing cells to transiently sustain therapeutic protein production *in situ*. In this study, a gene-activated NGC was developed by incorporating non-viral polyethyleneimine-plasmid DNA (PEI-pDNA) nanoparticles (N/P 7 ratio, 2µg dose) with the pDNA encoding for nerve growth factor (NGF), glial derived neurotrophic factor (GDNF) or the transcription factor c-Jun. The physicochemical properties of PEI-pDNA nanoparticles, morphology, size and charge, were shown to be suitable for gene delivery and demonstrated high Schwann cell transfection efficiency (60±13%) *in vitro*. While all three genes showed therapeutic potential in terms of enhancing neurotrophic cytokine production while promoting neurite outgrowth, delivery of the gene encoding for c-Jun showed the greatest capacity to enhance regenerative cellular processes *in vitro*. Ultimately, this gene-activated NGC construct was shown to be capable of transfecting both Schwann cells (S42 cells) and neuronal cells (PC12 and dorsal root ganglia) *in vitro*, demonstrating potential for future therapeutic applications *in vivo*.

Keywords: nerve guidance conduit; peripheral nerve repair; non-viral gene therapy

1. Introduction

Peripheral nerve transections occur in 2-3% of all trauma patients[1], requiring over half a million neurosurgical procedures to be carried out annually in the US [2]. When direct coaptation of the nerve endings is not possible, autografts are used to bridge the defect site, which can lead to permanent donor site morbidity and inadequate functional repair[3]. Nerve guidance conduits (NGCs), made from both synthetic and natural biomaterials, have emerged as an alternative treatment[4,5]. The basic requirements of biomaterial-based conduits have now been well established[5,6] and include providing macroscopic guidance between nerve endings, while being strong enough to withstand longitudinal tension and circumferential compression, in addition to being mechanically sound to facilitate surgical handling. Despite showing clinical success with the treatment of small injuries (< 15 mm)[7], the effective treatment of larger injuries with conduits poses an unmet clinical challenge[8,9]. To address this challenge, conduits have been used as platforms for the delivery of either cells[9-11], or growth factors[12-14] to enhance their regenerative capacity. Although encouraging, a lack of consensus on the ideal cell source and a dependency on controlled delivery systems[13,15-17] to avoid presenting cells with supraphysiological doses of growth factor[18,19] has limited the clinical translation of these approaches.

In this study, the potential to use a conduit as a platform for gene delivery is investigated. We have recently developed a biphasic NGC composed of a physicochemically optimized collagen-based outer conduit and a neuroconductive hyaluronic acid/laminin-based luminal filler[20], demonstrating its capacity to facilitate morphological and functional recovery across a 10 mm sciatic nerve injury in Sprague Dawley rats within 8 weeks[21]. More recent work from our group has shown that the addition of growth factors can enhance the regenerative capacity of existing biomaterials[22,23]. However, growth factor delivery for nerve repair poses substantial challenges owing to their short half-life *in vivo*[24], their limited temporal effect at the site of injury[25], and their potential to cause aberrant effects when used in supraphysiological doses[18,19]. Despite successful efforts by other labs to overcome some of these challenges by intricately controlling their delivery or by modifying their structure[13,15-17], protein delivery remains dependent on expensive therapeutics and delivery systems for high efficacy. In this context, the goal of this study was to

develop a gene-activated NGC, using our previously developed conduit as a platform for delivery[20] that incorporates polymer-based nanoparticles as non-viral (NV) vectors to carry therapeutic genes, and to assess the effects of gene delivery *in vitro*.

The gene-activated NGC proposed in this study is based on recent pioneering work in our lab that has led to the development of a series[26-30] of gene-activated scaffolds designed to transfect endogenous cells for a wide variety of applications, including accelerating bone and cartilage repair. This approach avoids presenting cells with supraphysiological doses of growth factors and takes advantage of host cells to produce therapeutic proteins. Focusing on a new clinical application with a distinct delivery platform, we envisage a gene-activated NGC to transfect endogenous Schwann cells as they migrate through the conduit so that they can produce therapeutic proteins, which might then have beneficial effects on Schwann cells but also on neuronal cells, potentially enhancing axonal outgrowth and repair. A major novelty of this approach lies in the fact that gene therapy approaches for peripheral nerve repair have typically focused on *ex vivo* genetic modification of Schwann cells for subsequent grafting[31], while our approach aims to deliver genes to endogenous cells *in situ*. A key determinant of success in this approach is the choice of gene delivery vector[32]. Viral vectors for example, which are widely used to genetically modifying Schwann cells *ex vivo* prior to grafting them[33,34], are associated with many disadvantages including the risk of insertional mutagenesis and the potential to elicit a strong immune response, which can lead to uncontrolled protein expression and aberrant peripheral nerve repair[18,19,31]. Therefore, NV gene delivery vectors can potentially overcome the limitations of viral vectors while providing sustained but transient and local gene expression[35]. However, efficient transfection of cells is a challenge with NV vectors and the lack of an established NV gene delivery vector to efficiently transfect Schwann cells is a major challenge for gene therapy and the development of a gene-activated NGC[36].

In this study, the cationic polymer polyethyleneimine (PEI) is utilized as a NV vector. PEI is a potent NV gene delivery vector that has been widely used both *in vitro* and *in vivo* since its first application as a transfection agent[37]. Previously, our group has optimized PEI-pDNA nanoparticles for transfection of bone marrow-derived mesenchymal stem cells although to the best of our knowledge[27], no studies have

evaluated PEI as a potential gene delivery vector for peripheral nerve repair. While PEI is renowned as a potent transfection agent[35], it is also well established that it can potentially render polymer-associated cytotoxicity[36], effects that are highly cell-specific and can be minimized through optimization[38,39]. This study evaluated its benefits and potential risks *in vitro* for peripheral nerve repair application.

Genes encoding for nerve growth factor (NGF)[40] and glial derived neurotrophic factor (GDNF)[41,42] were used in this study due to the bioactivity of the proteins they encode. NGF promotes the survival and axonal outgrowth of sensory neurons[43], while GDNF is an important survival factor of motor neurons and sensory neurons[44], and also stimulates the migration and proliferation of Schwann cells[41]. Genes encoding for these proteins have previously been used with varying success[45]. For example, permanent overexpression of GDNF by Schwann cells has led to enhanced repair in the short term, but ultimately aberrant effects including axonal trapping at the site of injury[18,19,46]. Although undesirable, these results demonstrate the promise of gene therapy and highlight the requirement of transient, non-permanent expression for high efficacy. Considering the potentially synergistic effects between NGF, GDNF and other neurotrophic factors[12,47], the transcription factor c-Jun encoded by JUN, which is involved in Schwann cell reprogramming in response to injury and the upregulation of multiple neurotrophic factors[48,49], presents another option that was investigated in this study for its potential to be more efficient than either genes encoding for NGF or GDNF.

The overall objective of this study was thus to ‘activate’ our previously developed conduit[5] with PEI-pDNA nanoparticles incorporating genes encoding for NGF, GDNF and c-Jun and to assess their effect on Schwann cells and neuronal cells *in vitro*. Specifically, we first evaluated the physicochemical properties of PEI-pDNA nanoparticles for gene delivery. Secondly, we assessed Schwann cell transfection efficiency in 2D monolayer. Thirdly, we assessed the biological response of Schwann cells, and neuronal cells, to the optimized PEI-pDNA nanoparticles carrying genes encoding for NGF, GDNF and c-Jun. Lastly, the optimized PEI-pDNA nanoparticles were incorporated into the luminal filler of the conduit[5] in order to assess Schwann cell transfection in the 3D microenvironment and the functionality of the gene-activated NGC in terms of its effect on Schwann cells and neuronal cells *in vitro*.

2. Materials and methods

2.1 Evaluation of the physicochemical properties of PEI-pDNA nanoparticles

2.1.1 Gene propagation

To evaluate PEI-pDNA nanoparticles, two reporter genes encoded into pDNA constructs were used in this study: pGreen Fluorescent Protein (pGFP) supplied by Amaxa, Lonza, Cologne, Germany, and p*Gaussia* luciferase (pGLuc), purchased from New England Biolabs, Massachusetts, USA. Therapeutic genes encoding human nerve growth factor (pNGF, accession number NM_002506), glial derived neurotrophic factor (pGDNF, accession number NM_199231), and c-Jun (pJUN, accession number NM_002228), were cloned into the multiple cloning site (MCS) of pcDNA3.1-C-eGFP plasmids (GenScript, Piscataway, NJ, USA) using BamH I and Not I restriction sites. The plasmid contains the DNA sequence coding for reporter GFP downstream of the MCS, and thus provides a quick means to verify whether transfection has been successful. All plasmids were propagated by transforming DH5α chemically competent *E. coli* cells according to the manufacturer's protocol (Cat # 18258012; Thermo Scientific, Ireland). The pDNA was then purified using Qiagen Endofree plasmid maxi kit as per manufacturer's instructions (Cat # 12362; Qiagen, Manchester, UK). Purified pDNA was subsequently quantified using Nanodrop 2000 spectroscopy. The plasmids were then diluted and used at a concentration of 0.5 µg/µL in TE buffer.

2.1.2 Nanoparticle formulation

25 kDa PEI (Cat # 408727; Sigma-Aldrich, Ireland), was complexed with anionic pDNA by electrostatic interaction at an N/P ratio of 7. PEI-pDNA nanoparticles were formulated carrying a 2 µg dose of pDNA[27]. Lipofectamine 2000™ (Cat # 11668019; Thermo Scientific, Ireland) was used as a control and formulated according to manufacturer's instructions. As PEI has previously been shown to be cytotoxic, 7.3 kDa chitosan (Novamatrix, Norway) nanoparticles, at an N/P ratio of 10 carrying a 2 µg dose of pDNA, were also tested[26].

2.1.3 Assessment of nanoparticle size and morphology

PEI-pDNA (N/P 7, 2 µg pDNA) and Lipofectamine 2000-pDNA nanoparticles (2 µg pDNA) formulated as previously described in *Section 2.1.2* without fixation and assessed with transmission electron microscopy (TEM) using a protocol adapted from the literature[50]. Briefly, samples (5 µL) were placed on a 200-mesh copper grid coated with silicon monoxide/formvar for 10 minutes. Excess sample was removed using Whatman filter paper. Negative staining was then carried out with 5 µL uranyl acetate (2%) for 2 minutes. Excess stain solution was removed by Whatman filter paper and the grid was dried at room temperature. Electron micrographs were taken with a Hitachi H7650 transmission electron microscope at an accelerating voltage of 100 kV. To determine the morphology and diameter of nanoparticles, post image analysis was carried out using Fiji (ImageJ) software[51].

2.1.4 Assessment of nanoparticle degradation characteristics

For efficient gene delivery *in vivo*, the vector should have the capacity to protect pDNA from enzymatic degradation. To assess this capacity, a DNA degradation assay was carried out. Nanoparticles were formulated as described in *Section 2.1.2*. $MgSO_4$ was added to a final concentration of 0.1 µM. Samples were incubated with 8 units of deoxyribonuclease I (DNase I) per 1 µg of pDNA for 30 minutes at 37 °C. Samples were loaded into a 1% agarose gel containing SYBRGreen (Cat # S7563; Thermo Scientific, Ireland) and run at 100 V for 2.5 h. The gel was imaged using AlphaImagerMini UV-transilluminator set to 365 nm. To determine the effect of enzymatic degradation, DNA banding patterns were assessed by post image analysis carried out using Fiji (ImageJ) software[51].

2.1.5 Assessment of nanoparticle complexation efficiency and stability

To determine complexation efficiency between PEI and pDNA in the formation of nanoparticles, an exclusion assay was carried out using SYBRSafe (Cat # S33102; Thermo Scientific, Ireland), which fluoresces upon binding to DNA. However, complexation with PEI prevents the dye from intercalating with DNA, thus ‘excluding’ it, and quenching fluorescence. Nanoparticles were formulated as described in *Section 2.1.2* and then diluted to 1.5 ml with 20 mM NaCl. SYBRSafe was then added and the fluorescent signal was measured with a spectrophotometer (Perkin Elmer LS 50B) at an excitation wavelength of 488 nm and an emission wavelength of 522 nm. The

complexation efficiency was estimated by calculating the ratio between the fluorescence measured from PEI-pDNA nanoparticle (N/P 7, 2 µg pDNA) samples and the fluorescence measured from an equivalent amount of non-encapsulated pDNA. Nanoparticle stability was then estimated by calculating the same as a function of time spent by the nanoparticles at 37 °C, thus the exclusion assay was carried out at various time points up to 28 days *in vitro*, to assess their long-term stability.

2.2 Assessment of PEI-pDNA nanoparticle transfection efficiency

2.2.1 Schwann cell (S42 cell line) culture

The rat Schwann cell line[52] (S42 cells) (Cat # CRL-2942; ATCC, Virginia, US), was used as a model of non-myelinating, pro-regenerative, endogenous Schwann cells, and were expanded in tissue culture plastic with DMEM (Cat # D5546; Sigma-Aldrich, Wicklow, Ireland) supplemented with 10% fetal bovine serum, 2mM L-glutamine and 1% penicillin-streptomycin, at 37°C and 5% CO_2. Their Schwann cell phenotype was verified using immunocytochemistry, staining for S100B and GFAP (*Supplementary 1*).

2.2.2 Neural progenitor cell (PC12 cell line) culture

The rat neural progenitor cell line[53] (PC12) (Cat # CRL-1721; ATCC, Virginia, US), was used as a model of neuronal cells, and were grown in collagen type-IV (0.1 mg/ml) (Cat # C5533; Sigma-Aldrich, Wicklow, Ireland) coated tissue culture plastic with RPMI-1640 medium (Cat # R0883; Sigma-Aldrich, Wicklow, Ireland) supplemented with 10% horse serum, 5% fetal bovine serum, 2mM L-glutamine and 1% penicillin-streptomycin, at 37°C and 5% CO_2. Their neuronal phenotype was verified using immunocytochemistry, staining for β-tubulin and neurofilament (*Supplementary 1*).

2.2.3 Dorsal root ganglia isolation and culture

For completeness, we also decided to assess the response of adult DRG, a mixed population of cells consisting of both Schwann cells and neuronal cells, and to determine whether the process of axonal outgrowth could be enhanced in the presence of PEI-pDNA nanoparticles loaded with therapeutic genes. DRG tissue isolated from adult male Wistar rats (285-350 g) was used in this study, and kindly donated by fellow researchers at the Tissue Engineering Research Group in keeping

with the 3Rs. Post-mortem tissue harvesting was approved by the RCSI Research Ethics Committee (REC1236). DRG were isolated according to a protocol adapted from Päiväläinen *et al.* 2008[54]. DRG were extracted from 3 rats, with 3 DRGs removed from each animal. Thus, n of 3 takes into account recordings from 9 DRGs. The spinal cord was placed in ice-cold PBS, and the DRG were identified and removed using tweezers. Nerve roots were trimmed as close as possible to the body of the DRG. Once isolated, DRG were placed in tissue culture wells and cultured with ice-cold neurobasal (NB) media (Cat # 21103049; Gibco, Ireland) containing N2 supplement (Cat # 17502001; Gibco, Ireland). Within an hour, DRG were placed in 37°C and 5% CO_2, and cultured in suspension overnight. 24-well plates were coated with Matrigel (Corning, Amsterdam, The Netherlands) diluted 1:4 in NB media. DRG were allowed to adhere to the bottom of the wells and cultured with 200 µl NB media overnight to promote attachment.

2.2.4 Transfection protocol

At 24 h prior to transfection, cells were seeded at a density of 13,000 cells/cm^2 in adherent well plates. The growth media was removed 1 hour pre-transfection and replaced with OptiMEM (Cat # 31985070; Gibco, Ireland). Nanoparticles were formulated as described in *Section 2.1.2* and following complexation, were mixed with OptiMEM and added to the cells. The transfection media was removed 4 hours post-transfection, cells were washed in PBS and cells were returned to growth media.

2.2.5 Assessment of the transgene expression and the transfection efficiency in transfected cells

To determine the transgene expression of transfected Schwann cells, the reporter gene pGLuc encoding for the luminescent protein luciferase was used. Nanoparticles were formulated as described in *Section 2.1.2* and Schwann cells were transfected as described in *Section 2.2.4*. Media samples from transfected cells were collected at 1, 3, 7, 14, 21 and 28 days post-transfection to assess transgene expression over a physiologically relevant timeframe. The luciferase in these samples was quantified using the Pierce *Gaussia* Luciferase Flash Assay Kit (Cat # 16158; Thermo Scientific, Ireland) following the manufacturer's instructions. To determine the percentage transfection efficiency of nanoparticles, pDNA encoding green fluorescent protein (pGFP) was used. Schwann cells were transfected with PEI-pGFP nanoparticles (N/P

7, 2 µg pGFP) and images of fluorescent cells expressing GFP were captured after 3, 7 and 14 days of culture with a Leica DMIL microscope to verify GFP expression (Leica Microsystems, Switzerland). The transfection efficiency was estimated as the percentage of GFP^+ cells in the population and quantified using flow cytometry with FACS Canto 11 DIVA software using day 3 as transfection efficiency percentage.

2.2.6 Evaluation of nanoparticle cytotoxicity

To assess cell proliferation post-transfection, a Quant-iT PicoGreen dsDNA assay kit (Cat # P11496; Life Sciences, Ireland) was used to quantify dsDNA concentration in transfected cells and compared to non-transfected cells. Lysis buffer (0.2 M carbonate buffer, 1% Triton X) was used to lyse cells, and the lysate was then assessed using the manufacturer's protocol. The dsDNA concentration was deducted using a standard curve and related to non-transfected cells as the 100% control. To assess metabolic activity post-transfection, the one step MTS Cell Proliferation assay (Cat # G3582; Promega, Ireland) was used according to manufacturer's instructions. Photometric absorbance at a wavelength of 490 nm was measured and related to that of non-transfected cells as the 100% control. Metabolic activity and dsDNA concentration assays were carried out after day 1, 3, 7 and 14 to determine if PEI had short-lived or permanent cytotoxicity effects.

2.3 Assessment of the cellular response to optimized nanoparticles carrying pNGF, pGDNF and pJUN

In order to assess the biological response to genes encoding for NGF, GDNF and c-Jun, optimized nanoparticles made up of PEI (N/P 7, 2 µg pDNA) and each therapeutic gene, were formulated as previously described in *Section 2.1.2* and used to transfect (i) Schwann cells (S42 cells), the target population *in vivo*, (ii) neural progenitor cells (PC12 cells) to assess the response of neuronal cells, which may potentially become transfected *in vivo*, and (iii) adult dorsal root ganglia (DRG) to assess the effect of transfection on a mixed cell population and the potential to enhance axonal outgrowth.

2.3.1 Assessment of the response of Schwann cells to pNGF, pGDNF and pJUN

To determine if Schwann cells (S42 cells) had been successfully transfected with pNGF, pGDNF and pJUN, GFP expression was assessed 7, 14 and 28 days post-

transfection using a Leica DMIL microscope (Leica Microsystems, Switzerland) to verify determine long-term therapeutic transgene expression. To assess the effect on Schwann cell growth and proliferation, metabolic activity (MTS) assays were carried out as previously described in *Section 2.2.6* on transfected cells after 7 days of culture and compared to non-transfected cells. To quantify the levels of therapeutic protein produced by Schwann cells in response to transfection, the levels of NGF, GDNF, CNTF, and myelin associated glycoprotein (MAG) were quantified using ELISAs following the manufacturer's instruction (Cat # DY556, DY212, DY557 and DY538; R&D Systems, UK) and compared to non-transfected cells. NGF and GDNF expression levels were assessed to confirm overexpression post-transfection, while CNTF, a promoter of neuronal survival and outgrowth, was assessed since it displays a limited increase in expression post-injury, and MAG was assessed because its expression level is inversely related to Schwann cell proliferation[25,52].

2.3.2 Assessment of the response of PC12 cells to pNGF, pGDNF and pJUN, and immunofluorescence staining

PC12 cells were transfected as described in *Section 2.2.4*, and assessed for neurite outgrowth 7 days post-transfection. Neurite outgrowth assays were carried out in 24-well plates at a seeding density of 25,000 cells/cm^2. The functional bioactivity of gene products was validated by assessing the autocrine (*i.e.* GFP$^+$ cells with neurite outgrowth) and paracrine-mediated (*i.e.* GFP$^-$ cells with neurite outgrowth) induction of neurite outgrowth. Immunofluorescence staining was carried out to identify neurite outgrowth (β-tubulin III) and c-Jun expression post-transfection as these cells do not natively express it, while a nuclear stain Hoechst 33258 was used for counterstaining. Briefly, samples were incubated with rabbit anti-β-tubulin III (200kDa) or rabbit anti-c-Jun (Cat # ab18207 and ab32137; Abcam, Cambridge, UK) at 1:200 dilutions following cell fixation with 10% formalin (1 hour), and permeabilization with 0.1% Tween20 (30 minutes). Alexa Fluor 546 anti-rabbit secondary antibody (Cat # A-11035, Thermo Scientific, Ireland) was used at 1:500 dilution (2 hour incubation) and Hoechst 33258 was added as per manufacturer's instruction (10 minutes incubation) (Cat # 861405; Sigma-Aldrich, Wicklow, Ireland) and samples were washed prior to imaging.

2.3.3 Assessment of the response of adult DRG to pNGF, pGDNF and pJUN

After successful attachment (24 hours), DRG were transfected as described in *Section 2.2.4*. Axonal outgrowth was assessed using immunofluorescence staining for β-tubulin III 14 days post-transfection, as longer timepoints are unsuitable for DRG culture. The length of axonal outgrowth from transfected DRG was then quantified by post-image analysis using Simple Neurite Tracer Fiji (ImageJ) plugin[51,55] in comparison to that of non-transfected DRG to assess enhanced growth.

2.4 Fabrication of a gene-activated NGC and assessment of Schwann cell transfection in 3D

2.4.1 Fabrication of a gene-activated NGC

To fabricate a gene-activated NGC, the optimized PEI-pDNA nanoparticles were incorporated into the hyaluronic acid (HyA)-based luminal filler of our previously developed NGC as a model natural polymer-based conduit[20] via a soak-loading technique that has been used in our lab to successfully gene-activate collagen-based scaffolds for osteochondral repair[26,27,29]. To determine whether transgene expression could be recapitulated in 3D, nanoparticles carrying pGLuc were incorporated into the NGC. Samples of HyA luminal filler (1 cm^2 x 4 mm) were prepared as described in our previous study[20] and PEI-pGLuc nanoparticles (N/P 7, 2 μg pDNA) were incorporated by soak-loading directly onto the material following complexation. After a 15 minute incubation at room temperature, 5 x 10^5 Schwann cells (S42 cell line) were seeded onto gene-activated samples in OptiMEM and incubated for 4 hours at 37 °C, and then returned to growth media in order to assess *in vitro* whether the gene-activated NGC might lead to transient gene expression (*Schem. 1)*. Conditioned culture media was collected after 3, 7, 10, 14, 21, and 28 days of culture and evaluated using the luciferase assay described in *Section 2.2.5*.

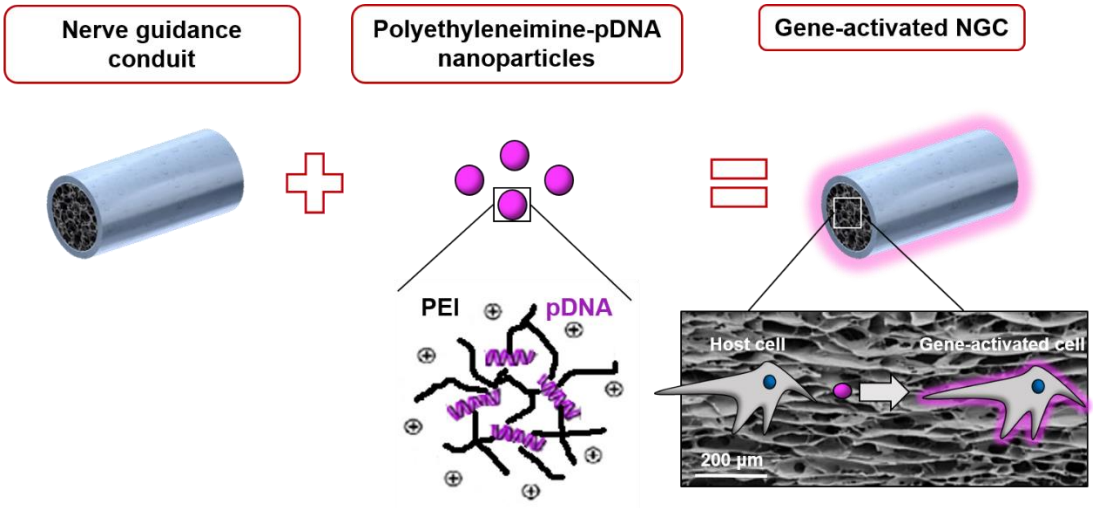

Schematic 1: Gene-activated nerve guidance conduit
Schematic of the gene-activated nerve guidance conduit composed the conduit and PEI-pDNA nanoparticles, which are incorporated into the luminal filler. First inset shows interaction between the positively charged polymer and the negatively charged pDNA, while second inset shows envisaged take up of nanoparticles by host cells as they migrate through the porous luminal filler, resulting in gene-activated cells.

2.4.2 Functional assessment of the gene-activated NGC

A series of gene-activated NGCs were prepared by incorporating PEI-pDNA nanoparticles (N/P 7, 2µg pDNA) carrying either pNGF, pGDNF or pJUN, in the luminal filler of the biphasic NGC previously developed in our research group[20]. Schwann cells (S42 cell line) were seeded on the gene-activated luminal fillers to assess transfection with pNGF, pGDNF and pJUN in 3D, and to assess the paracrine effects of transfected Schwann cells on PC12 cells as described in *Section 2.3.2*. GFP expression was assessed in 3D to verify that Schwann cells had been successfully transfected in the gene-activated luminal fillers with each of the three genes. The culture media was collected 14 days after transfection in 3D to quantify the NGF and GDNF production levels using ELISA kits following the manufacturer's instruction (R&D Systems, UK) as described in *Section 2.3.1*. A neurite outgrowth assay was then carried out on PC12 cells using this culture media collected after 3, 7 and 14 days to determine the paracrine effect of transfected Schwann cells in 3D as described in *Section 2.3.2*.

2.5 Statistical analysis

Results are expressed as mean ± standard deviation. In *Figures 3C, 4C, 5C, 6B and Supplementary B* statistical significance was assessed using one-way ANOVA

followed by Tukey post-hoc analysis. In the case of *Figures 2A, 2B, 2C, 3B and Supplementary A* two-way ANOVA analysis was carried out followed by Bonferroni post-hoc analysis. The sample size was n=3, unless stated otherwise, and $p \leq 0.05$ values were considered statistically significant where * $p<0.05$, ** $p<0.01$, *** $p<0.001$ and **** $p<0.0001$.

3. Results

3.1 Evaluation of the physicochemical properties of PEI-pDNA nanoparticles

The physicochemical properties of the PEI-pDNA nanoparticles were assessed to ensure that they meet precise standards in order to have high efficiency: they should have a diameter of approximately 100 nm, carry a positive charge, protect pDNA from enzymatic degradation, and they should have a high complexation efficiency and stability over time.

The zeta potential of PEI-pDNA nanoparticles with a range of N/P ratios has previously been determined[27], and nanoparticles with N/P 7, carrying 2 µg of pDNA, were shown to have a zeta potential of approximately +30 mV[56] rendering them suitable for cellular uptake by Schwann cells, which have a membrane potential of approximately -70 mV. To ensure they meet the size threshold of approximately 100 nm for cell uptake, PEI-pDNA nanoparticles (N/P 7, 2 µg pDNA) were prepared and visualized using TEM and compared to Lipofectamine 2000-pDNA nanoparticles in terms of morphology and size (*Fig. 1A*). TEM analysis showed that homogenous nanoparticle formation is achievable with PEI, generating nanoparticles with an average diameter of 40±10 nm and a regular, spherical morphology. In comparison, using Lipofectamine 2000 resulted in more irregular nanoparticles with an average diameter of 56±15 nm and a much less defined morphology, with supercoiled pDNA found protruding from some nanoparticles, suggesting that pDNA was poorly retained. To ensure efficacy, pDNA should be protected from enzymatic degradation until it is taken up by cells. When PEI's capacity to protect pDNA from enzymatic degradation was assessed, results showed that incubation with deoxyribonuclease I (DNase I) for 30 minutes at 37 °C was sufficient to completely degrade free pDNA as suggested by the lack of banding formation in gel electrophoresis (*Fig. 1B, Lane 3*) compared to the typical pDNA banding pattern (*Fig. 1B, Lane 2*). In contrast, pDNA complexed with PEI was retained in wells (*Fig. 1B, Lane 4*), suggesting a high complexation efficiency between PEI and pDNA. Nanoparticles incubated with DNase I for 30 minutes prior to loading resulted in the same banding pattern (*Fig. 1B, Lane 5*), suggesting that PEI can protect pDNA from enzymatic degradation. In terms of complexation efficiency between PEI and pDNA, an initial complexation efficiency of 92% was recorded

immediately after nanoparticle formation. After 28 days incubation at 37 °C, in excess of 90% of the initial pDNA dose was still in complex with PEI, highlighting the stability of these nanoparticles at 37 °C (*Fig. 1C*).

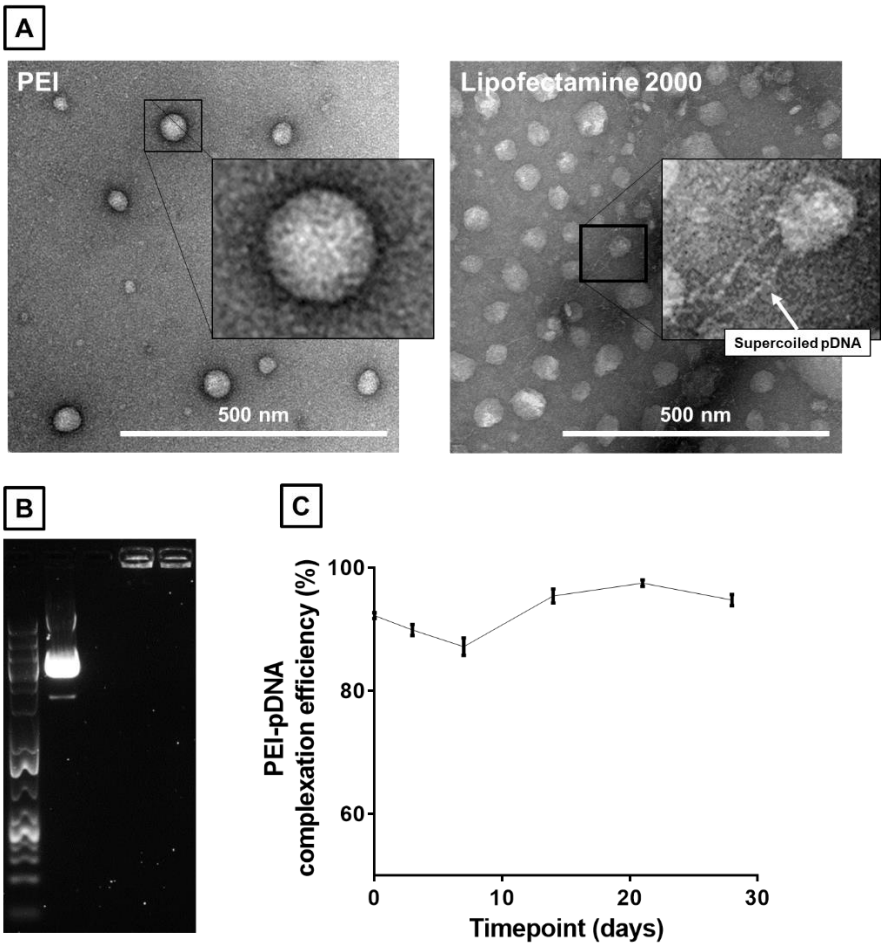

Figure 1: Physicochemical characterization of PEI-pDNA nanoparticles
A) TEM images of PEI-pDNA nanoparticles and Lipofectamine 2000-pDNA nanoparticles. PEI-pDNA nanoparticles had a smooth and round morphology in contrast to Lipofectamine 2000-pDNA nanoparticles, which had an irregular morphology and showed evidence of disassociation between supercoiled pDNA and the polymer. The average diameter of PEI-pDNA and Lipofectamine 2000-pDNA nanoparticles was 40 and 56 nm, respectively. B) Image of agarose gel showing that PEI renders protection to pDNA from enzymatic degradation suggested by the banding pattern after digestion with DNase. C) Complexation efficiency between PEI and pDNA expressed as a function of time, showing the stability of the nanoparticles over time. Data plotted represents mean ± standard deviation, n = 3.

3.2 Assessment of PEI-pDNA nanoparticle transfection efficiency

Schwann cells (S42 cells) were transfected with PEI-pGLuc nanoparticles (N/P 7, 2 µg pGLuc) to determine transgene expression and compared to transfection using Lipofectamine 2000-pGLuc. Luciferase expression was evaluated for 28 days after transfection with pGLuc, and transient expression profiles were obtained for both

vectors and compared to non-transfected cells (*Fig. 2A*). Cells transfected using PEI-pGLuc led to significantly higher ($p<0.0001$) transgene expression compared to cells transfected using Lipofectamine 2000, with significant differences in expression observed at 3 and 7 days post-transfection. Based on these transgene expression results, Lipofectamine 2000 was not carried further into the study.

To determine if the PEI-pGLuc nanoparticles negatively affected Schwann cell viability post-transfection, DNA quantification and metabolic activity assays were carried out. Results suggest that PEI had a negative impact on cell proliferation within 3 days of transfection (*Fig. 2B*), with cells proliferating on average 21% ($p<0.0001$) less than non-transfected cells after 7 days. However, the effect of PEI on cell proliferation became less significant ($p<0.01$) 14 days post-transfection, with only a 14% lower level in cell proliferation compared to non-transfected cells. Moreover, results show that cells had 30% ($p<0.0001$) lower metabolic activity 3 days after being transfected with PEI compared to non-transfected cells, and an even lower level after 7 days ($p<0.0001$) (*Fig. 2C*). Despite this, cells showed increased metabolic activity 14 days post-transfection compared to earlier timepoints, with less significance difference compared to non-transfected cells ($p<0.001$).Taken together, these results suggest that PEI-pDNA nanoparticles had a limited cytotoxic effect following Schwann cell transfection in 2D, lowering both their proliferation and metabolic activity immediately after transfection but without long-term effects, and well within the maximum accepted toxicity of 35% in 2D transfections[27]. Due to the significant reduction in cell viability caused by the PEI-pDNA nanoparticles, a vector known to have limited cytotoxicity issues, chitosan, was tested at a formulation previously optimised for mesenchymal stem cell transfection (N/P 10, 2 µg pDNA). However, the low transfection efficiency of <5% was deemed unsuitable so chitosan was not used for further studies (*Supplementary 2A*).

In order to quantify the transfection efficiency, Schwann cells (S42 cells) were transfected with pDNA encoding GFP. Fluorescent green cells were found throughout transfected cultures, indicating successful transfection with GFP (*Fig. 2D*). Quantification of these results show that peak Schwann cell transfection efficiency is 60±13%, and a reduction in GFP^+ cells over time suggests that their transgene expression is transient as desired. Additionally, we tried to optimize the transfection

efficiency by increasing the pDNA dose but found that this led to increasing cytotoxicity due to increased PEI concentration necessary to maintain the N/P ratio constant (*Supplementary 2B*). Collectively, these findings suggest that the optimal nanoparticle formulation consists of PEI-pDNA nanoparticles carrying a 2 µg dose of pDNA with an N/P ratio of 7.

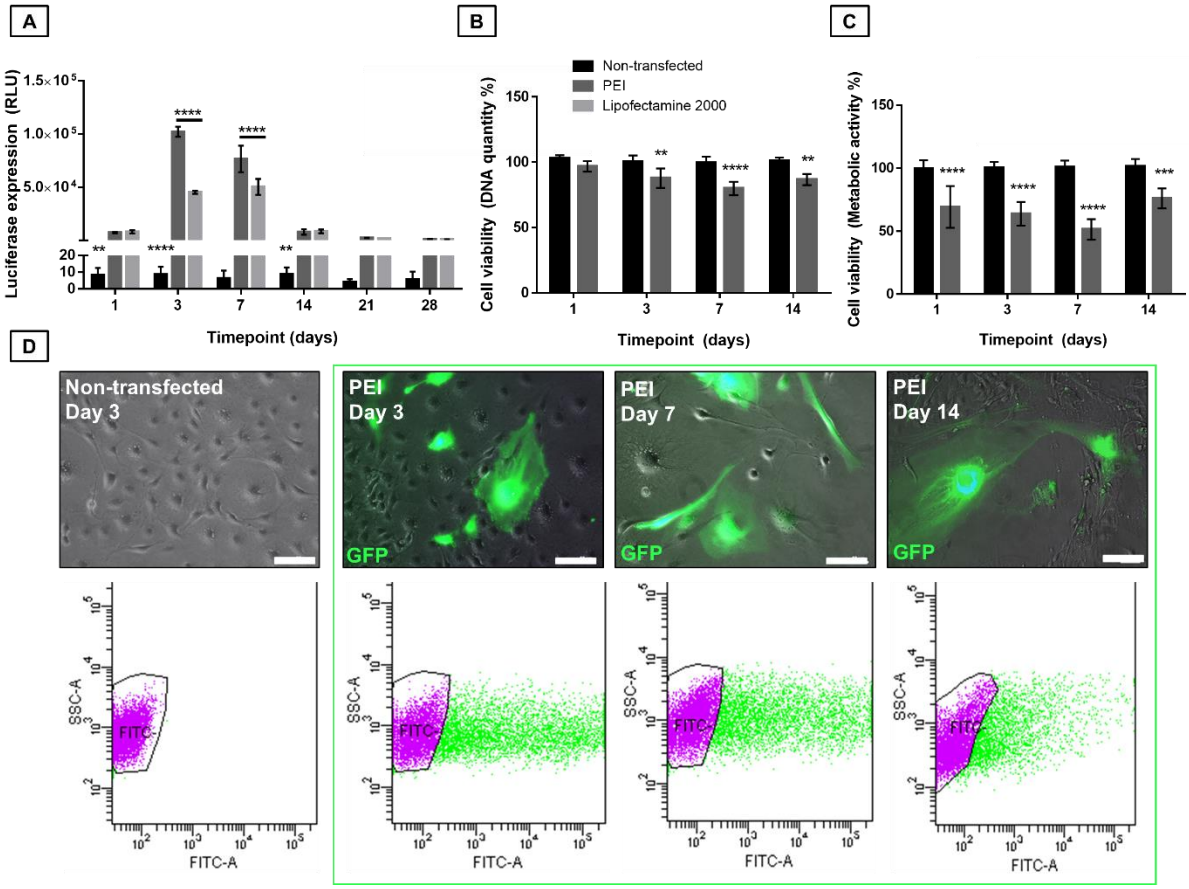

Figure 2: Assessment of transfection efficiency
A) *Gaussia* Luciferase gene expression as a function of time in Schwann cells transfected with PEI-pGLuc and Lipofectamine 2000-pGLuc nanoparticles compared to non-transfected cells. Both vectors rendered a transient gene expression profile compared to non-transfected cells, however, PEI led to significantly higher gene expression than Lipofectamine 2000, 3 and 7 days after transfection. B) Schwann cell viability following transfection with PEI in terms of DNA quantity and C) metabolic activity, suggesting that PEI-mediated cytotoxicity is limited and does not last long-term. D) Fluorescent microscopy images superimposed over brightfield images showing examples of cells expressing GFP in comparison to non-transfected cells up to day 14, scale bar 100 µm. Flow cytometry reported a transfection efficiency of 60±13% 3 days post-transfection, while flow cytometry side scatter plots show a decrease in GFP^+ cells over time. Data plotted represents mean ± standard deviation, n = 3. **, *** and **** denotes $p<0.01$, $p<0.001$ and $p<0.0001$, respectively, two-way ANOVA.

3.3 Assessment of the cellular response to PEI nanoparticles carrying pNGF, pGDNF and pJUN

Having determined that PEI-pDNA nanoparticles are capable of transfecting Schwann cells (S42 cells), we next sought to assess the effects of delivering genes encoding for therapeutic proteins. Schwann cells were transfected with PEI nanoparticles carrying pNGF, pGDNF and pJUN coding for NGF, GDNF and c-Jun, respectively. Fluorescent green Schwann cells (GFP^+) were evident throughout transfected cultures suggesting that they had been successfully transfected with each of the three genes (*Fig. 3A*). Moreover, some Schwann cells were found to be GFP^+ up to 28 days after transfection, suggesting that therapeutic protein production was, although transient, sustained for sufficient time to potentially have a beneficial effect in a peripheral nerve repair application. The viability of Schwann cells post-transfection was assessed and results suggest that each of the three genes were capable of mitigating PEI-associated cytotoxicity (*Fig. 2C*), with transfected cells showing no significant difference in metabolic activity compared to non-transfected cells 7 days post-transfection *(Fig. 3B*).

Having determined that there was no significant difference in metabolic activity between non-transfected cells and Schwann cells transfected with each PEI complex (N/P 7, 2 µg pDNA), the expression of cytokines NGF, GDNF, CNTF and MAG, were next assessed at the same time-point (*Fig. 3C*). Transfection with pNGF led to a significant increase in NGF expression ($p<0.001$) and also a slight increase in GDNF expression ($p>0.05$). Similarly, transfection with pGDNF led to a significant increase in GDNF expression ($p<0.01$) and also an increase in NGF expression ($p<0.01$). Transfection with pJUN led to a significant increase in NGF production ($p<0.05$), and also an increase in GDNF production ($p>0.05$). Additionally, transfection with pNGF, pGDNF and pJUN led to a slight increase in CNTF expression ($p>0.05$), while also supressing MAG expression ($p<0.001$). Results suggest that while pJUN does not directly encode for neurotrophic cytokines, the transcription factor it encodes for, c-Jun, led to the overexpression of neurotrophic factors NGF, GDNF and CNTF, while also downregulating MAG.

Having determined that PEI-pDNA nanoparticles can efficiently deliver therapeutic genes to Schwann cells (S42 cells), we next sought to assess their potential effect on

neuronal cells. Results showed that PC12 cells could be successfully transfected with each gene, leading to neurite outgrowth in contrast to non-transfected cells, which retained a rounded cell morphology, thus suggesting that the neurotrophic cytokines encoded by these genes were functionally bioactive (*Fig. 3D*). Moreover, only cells transfected with pJUN were found to be c-Jun^{+}, confirming that the expression of c-Jun led to the production of neurotrophic cytokines, which in turn led to neurite outgrowth by both autocrine and paracrine means.

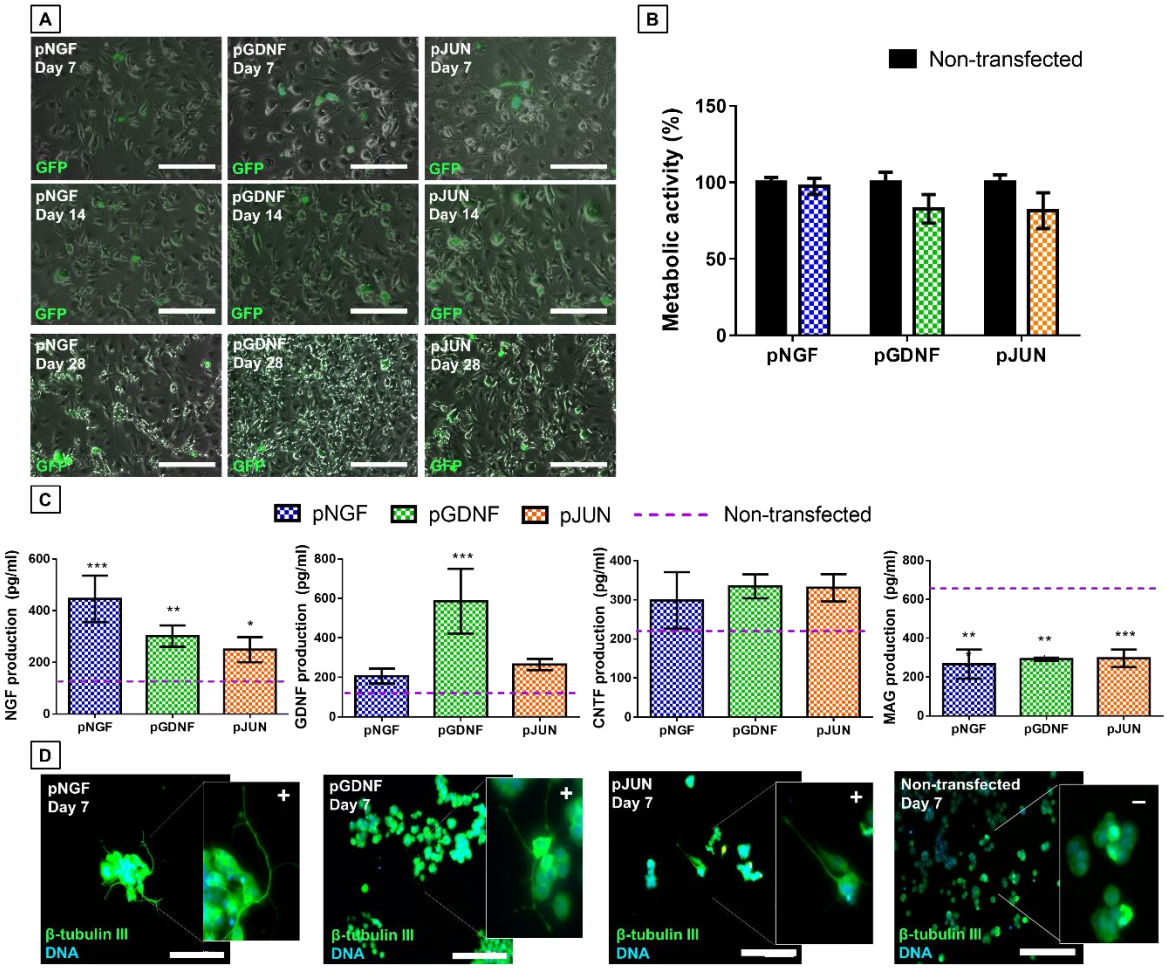

Figure 3: Assessment of the response of Schwann cells and PC12 cells to PEI-pDNA nanoparticles carrying pNGF, pGDNF and pJUN

A) Fluorescent microscopy images superimposed over brightfield revealing green fluorescent Schwann cells (GFP^{+}) in all groups up to 28 days post-transfection, suggesting that Schwann cells were successfully transfected with PEI-pNGF, PEI-pGDNF and PEI-pJUN (N/P 7, 2 µg pDNA), scale bar 100 µm. B) Schwann cell metabolic activity was assessed 7 days post-transfection in cells transfected with PEI-pNGF, PEI-pGDNF and PEI-pJUN, compared to non-transfected cells suggesting that the gene products are mitigating PEI-associated cytotoxicity. Data plotted represents mean ± standard deviation, n = 3. Two-way ANOVA. C) The expression levels of NGF, GDNF, CNTF and MAG were assessed in transfected cells after 7 days of culture and compared to baseline levels of expression in non-transfected cells, indicated with a dashed line, showing desired overexpression of neurotrophic cytokines. n =

3. *, **, *** and **** denote $p<0.05$, $p<0.01$, $p<0.001$, and $p<0.0001$, respectively, one-way ANOVA. D) Fluorescent microscopy images of PC12 cells with insets highlighting β-tubulin III^+ neurite outgrowth 7 days post-transfection, suggesting that PC12 cells could be transfected with PEI-pNGF, PEI-pGDNF and PEI-pJUN, and that the gene products are functionally bioactive, compared to non-transfected cells where neurite outgrowth was not reported, scale bar 200 µm.

For completeness, we also decided to assess the response of adult DRG, a mixed population of cells consisting of both Schwann cells and neuronal cells, in addition to fibroblasts and satellite glial cells, to each gene, and to determine whether axonal outgrowth could be enhanced. Results suggest that DRG were successfully transfected with each gene, indicated by the presence of bright green GFP^+ fluorescent DRG cells at 7 days post-transfection compared to non-transfected cells (*Fig. 4A*). Despite not being able to determine which particular cell type had been successfully transfected, we did some axonal β-tubulin III^+ outgrowth to be GFP^+ 14 days post-transfection (*Fig. 4B*), suggesting that sensory neurons can potentially also be transfected using PEI-pDNA nanoparticles, and that transgene protein production is also sustained. Moreover, we found that transfection with PEI-pNGF and PEI-pGDNF led to significantly longer axonal outgrowth compared to non-transfected DRG ($p<0.05$). Interestingly, transfection with PEI-pNGF and PEI-pGDNF nanoparticles leads to 1.9-fold longer axonal outgrowth compared to non-transfected DRG ($p<0.05$), but transfection with PEI-pJUN led to enhanced axonal outgrowth compared to all groups, 2.8-fold longer compared to non-transfected DRG ($p<0.001$), and 1.5-fold longer compared to DRG transfected with PEI-pNGF or PEI-pGDNF ($p<0.05$) (*Fig. 4C*).

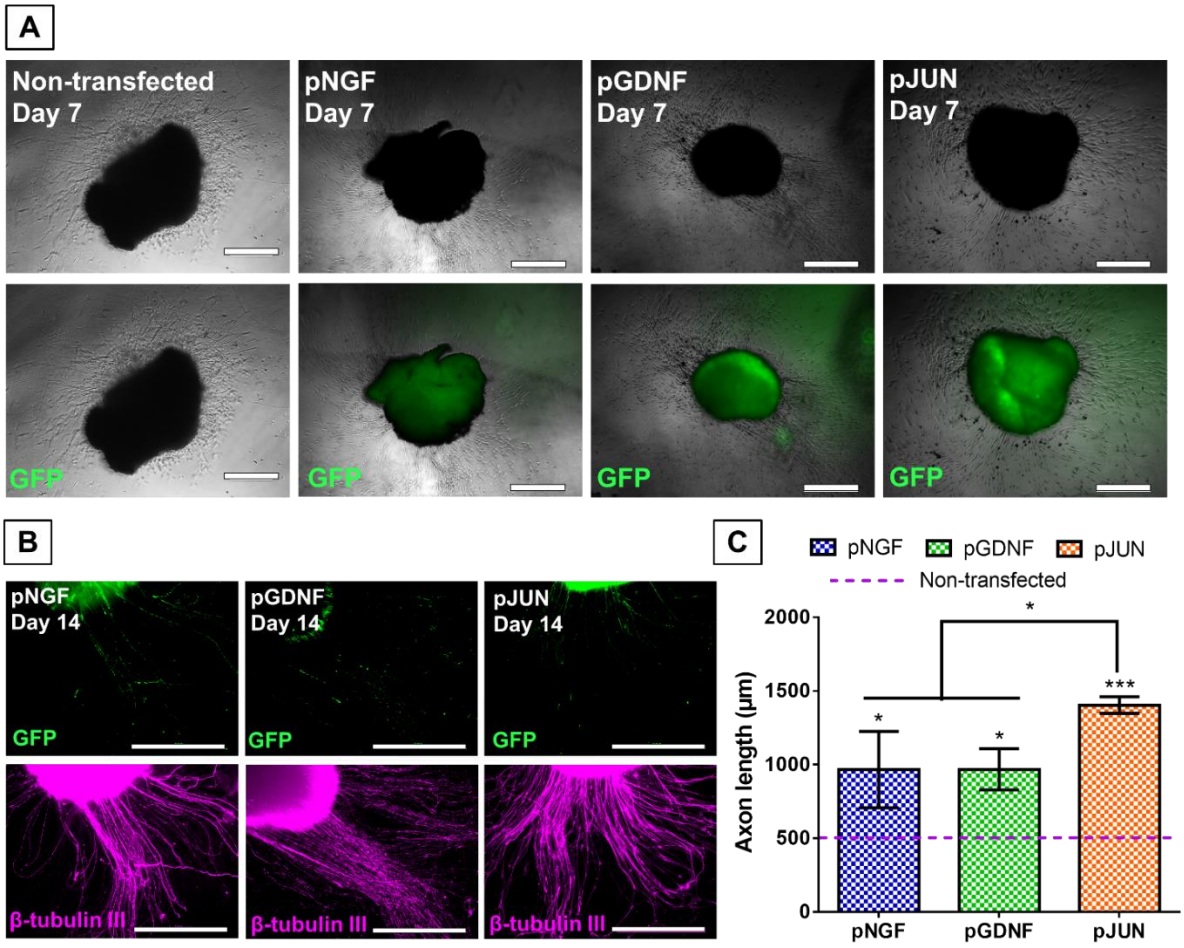

Figure 4: Assessment of the response of adult DRG to PEI-pDNA nanoparticles carrying pNGF, pGDNF and pJUN

A) Fluorescent microscopy images superimposed over brightfield shows GFP^+ cells in all transfected DRG compared to non-transfected after 7 days, suggesting they had been successfully transfected with PEI-pNGF, PEI-pGDNF and PEI-pJUN (N/P 7, 2 µg pDNA), scale bar 500 µm. B) Images of samples post-immunofluorescence carried out 14 days post-transfection, showing successfully transfected neuronal cells (GFP^+) and axonal outgrowth (β-tubulin III^+), scale bar 500 µm. C) Quantification of axonal outgrowth in transfected DRG, demonstrating that transfection with PEI-pNGF and PEI-pGDNF nanoparticles leads to 1.9-fold longer axonal outgrowth compared to non-transfected DRG, but transfection with PEI-pJUN led to enhanced axonal outgrowth compared to all groups, 2.8-fold longer compared to non-transfected DRG, and 1.5-fold longer compared to DRG transfected with PEI-pNGF or PEI-pGDNF. Data plotted represents mean ± standard deviation, n = 3. * and *** denote $p<0.05$ and $p<0.001$, respectively, one-way ANOVA.

3.4 Fabrication of a gene-activated NGC and assessment of Schwann cell transfection in 3D

We next sought to assess the effect of these genes in a 3D microenvironment within a NGC. First, we found that PEI-pDNA nanoparticles carrying genes encoding for luciferase could be seamlessly incorporated into the luminal filler of the biphasic NGC developed previously to create a gene-activated luminal filler. Results suggest that

luciferase expression by Schwann cells in the gene-activated luminal filler have a sustained but transient expression profile, similar in comparison to 2D, with an early peak in luciferase expression 3 days post-transfection followed by a slow and sustained reduction in transgene expression up to day 28 as desired (*Fig. 5A*). Schwann cells (S42 cells) were then successfully transfected in luminal fillers activated with each gene, suggested by the presence of GFP^+ cells found throughout the 3D microenvironment 3 days post-transfection (*Fig. 5B*). The levels of neurotrophic cytokine production by Schwann cells in the gene-activated luminal filler were significantly higher than the levels expressed by cells in the gene-free luminal filler (*Fig. 5C*). While the luminal filler activated with either PEI-pNGF and PEI-pGDNF led to enhanced levels of NGF ($p<0.01$) and GDNF ($p<0.001$) expression respectively, the luminal filler activated with PEI-pJUN led to greater levels of both NGF ($p<0.01$) and GDNF ($p<0.0001$) expression in comparison to both other groups after 14 days.

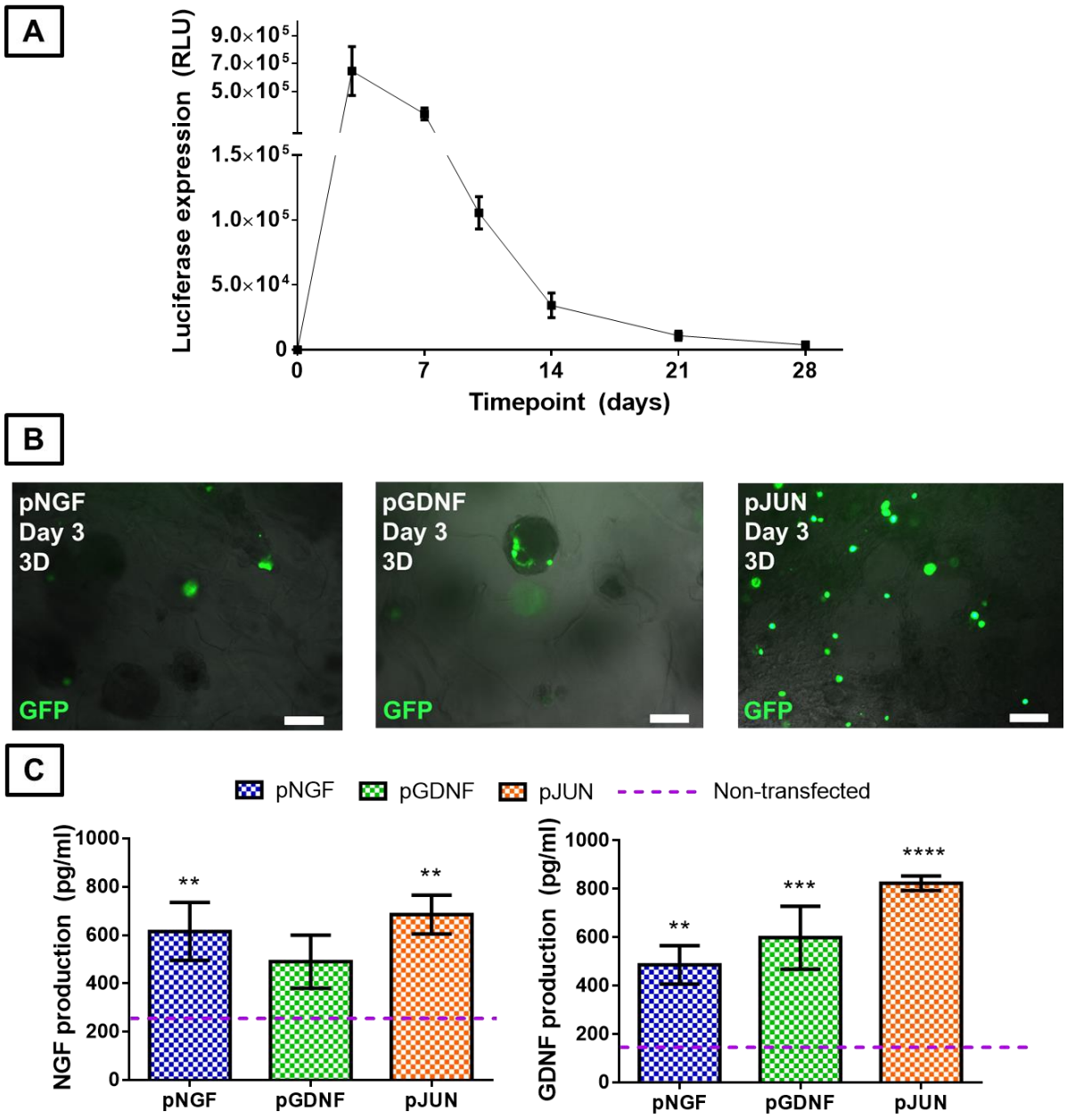

Figure 5: Assessment of Schwann cell transfection in gene-activated NGC
A) *Gaussia* Luciferase gene expression was monitored over 28 days from Schwann cells transfected with PEI-pGLuc nanoparticles (N/P 7, 2 µg pDNA) in the gene-activated luminal filler. Gene expression was transient over 28 days, peaked 3 days post-transfection, and followed the same trend as previously observed in 2D experiments. Data plotted represents mean ± standard deviation, n = 3. B) Schwann cells were transfected in luminal fillers activated with PEI-pNGF, PEI-pGDNF and PEI-pJUN. Fluorescence imaging showing representative images of successfully transfected GFP^+ Schwann cells in the gene-activated luminal fillers after 3 days. C) Quantification of the levels of NGF and GDNF expressed by Schwann cells in gene-activated luminal fillers after 14 days compared to the levels expressed by cells in the gene-free luminal filler (dashed line), showed that PEI-pJUN led to enhanced levels of neurotrophic cytokine production in 3D compared to all other groups. Scale bar 100 µm. Data plotted represents mean ± standard deviation, n = 3. **, *** and **** denote $p<0.01$, $p<0.001$, and $p<0.0001$, respectively, one-way ANOVA.

We next sought to assess the paracrine effect of Schwann cells (S42 cells) transfected within the gene-activated luminal fillers on neurite outgrowth. We found that conditioned media from each of the gene-activated luminal fillers, collected 3, 7 and 14 days after seeding Schwann cells on the constructs, was capable of inducing neurite outgrowth from PC12 cells compared to conditioned media from gene-free luminal filler, which had very low concentrations of neurotrophic cytokines and was incapable of inducing any neurite outgrowth (*Fig. 6A*). This thus demonstrates the sustained, paracrine effect of transfected Schwann cells in the gene-activated luminal filler on neurite outgrowth. Notably, conditioned media collected from the luminal filler activated with PEI-pJUN led to the most significant enhancement ($p<0.01$) in terms of neurite outgrowth per cell at each time point, suggesting again that the transcription factor c-Jun has the greater therapeutic potential than either genes encoding for NGF or GDNF (*Fig. 6B*).

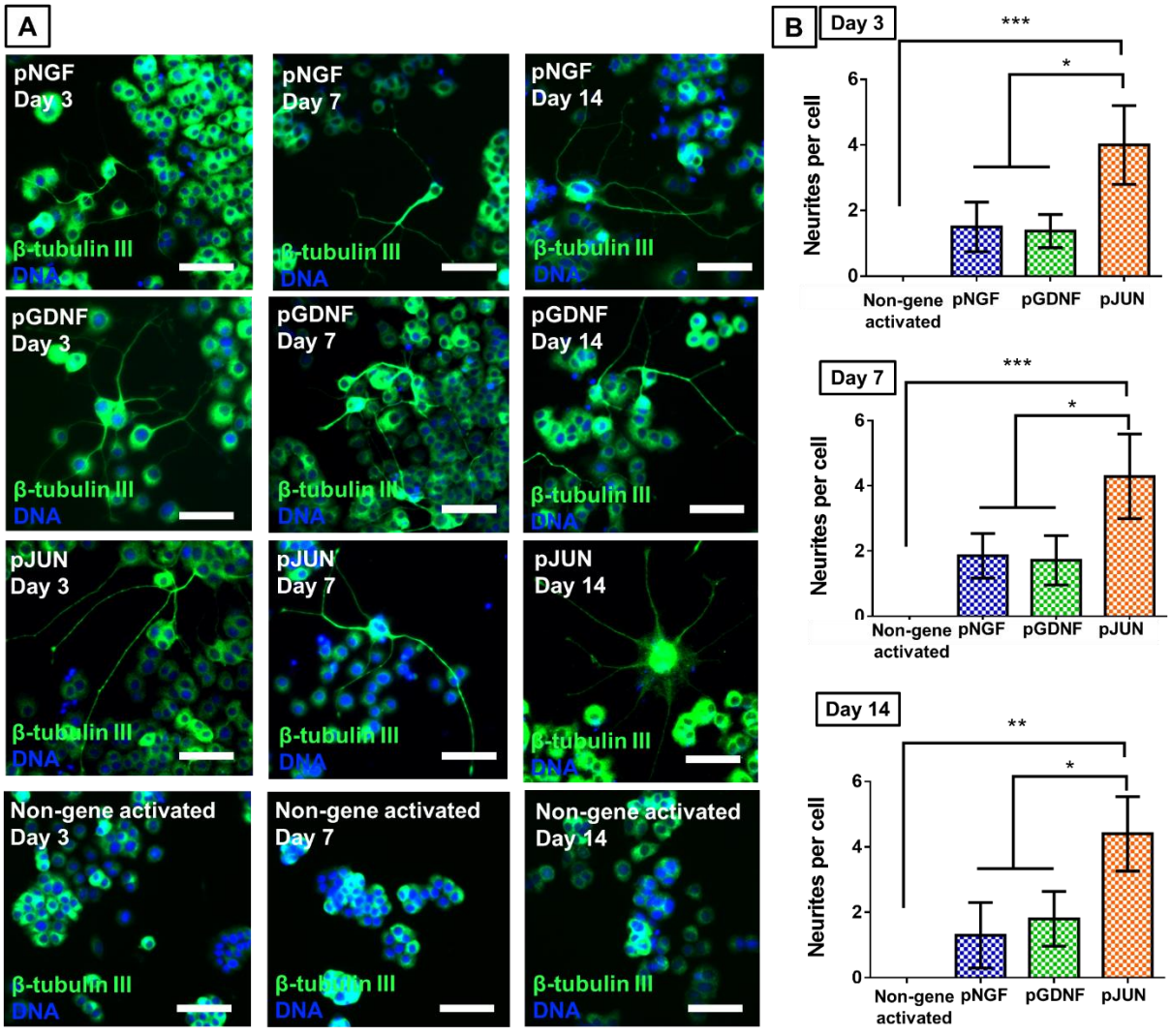

Figure 6: Paracrine effect of Schwann cells transfected in gene-activated luminal filler on neurite outgrowth

A) Neurite outgrowth from PC12 cells after 7 days in response to conditioned media collected from luminal fillers activated with PEI-pNGF, PEI-pGDNF and PEI-pJUN, 3, 7 and 14 days after seeding Schwann cells on them, compared to conditioned media from gene-free luminal filler (control). Cells are stained with β-tubulin III to highlight neurite outgrowth and Hoechst 33258 to depict cell nuclei. Scale bar 100 μm. B) The conditioned media from luminal filler activated with PEI-pJUN led to enhanced neurites per cell at each time-point compared to luminal filler activated with either PEI-pNGF or PEI-pGDNF, and gene-free luminal filler, highlighting the greater therapeutic potential of c-Jun. Data plotted represents mean ± standard deviation, n = 3. *, ** and *** denote $p<0.05$, $p<0.01$ and $p<0.001$, respectively, one-way ANOVA.

4. Discussion

In this study, a gene-activated NGC was developed, and assessed *in vitro*, by incorporating NV PEI-pDNA nanoparticles encoding for therapeutic genes into the luminal filler of the biphasic NGC developed previously[20]. This platform demonstrated the capacity to efficiently deliver genes encoding for therapeutic proteins, NGF, GDNF and c-Jun and elicit a beneficial response from Schwann cells and neuronal cells *in vitro*. The gene encoding for c-Jun was found to have greater effects in terms of enhancing pro-regenerative cell activity, including neurotrophic factor production and axonal outgrowth, than genes encoding for either neurotrophic factors. Ultimately, the ability of a gene-activated NGC to deliver pDNA was demonstrated *in vitro* resulting in a conduit that could elicit sustained but transient levels of enhanced neurotrophic protein production over time, which can lead to beneficial paracrine effects such as promoting neurite outgrowth.

While viral gene therapy for the correction of genetic disorders has led to recent successes[57-59], the main hurdle facing NV gene therapy for tissue engineering, and the development of a gene-activated NGC for peripheral nerve repair, is the lack of an efficient NV gene delivery vector[31]. In this study, pDNA was complexed with PEI with an N/P ratio of 7 and carrying 2 µg of pDNA to form PEI-pDNA nanoparticles of suitable size, morphology and charge for gene delivery. Previous studies have shown that the physicochemical properties of PEI-pDNA nanoparticles are a key determinant of gene delivery success[60,61]. The characteristics of the PEI-pDNA nanoparticles used in this study, with an average diameter of 40 nm and an overall cationic charge of +30mV, meet the criteria for efficient cell uptake. Although the mechanism of entry into the cell remains unknown, the combination of these properties potentially promotes nanoparticle binding to syndecans[62], which are negatively charged heparan sulfate proteoglycans in cell membranes, and subsequent internalization via endocytic vesicles[63]. Additionally, the findings from this study suggest that PEI protects pDNA from DNase degradation while maintaining its stability long-term for up to 28 days. These properties are also highly advantageous considering that transfection within a gene activated NGC is envisaged to be spaced out over time, *i.e.* as Schwann cells come into contact with nanoparticles as they migrate throughout the length of the luminal filler. Furthermore, morphology analysis revealed that PEI-pDNA

nanoparticles retained their structural integrity in contrast to Lipofectamine 2000-pDNA nanoparticles, which showed evidence of dissociation. Other studies corroborate our findings, suggesting that PEI-pDNA nanoparticles are also highly stable in human serum, and only aberrant conditions such as alkaline pH and high heparin content are capable of dissociating pDNA from PEI[64]. Taken together, these findings suggest that the physicochemical properties of PEI-pDNA nanoparticles are highly suitable for gene delivery in neural applications.

Despite their NV nature, PEI-pDNA nanoparticles were found to be highly efficient at transfecting Schwann cells (S42 cells) with an efficiency of 60±13%. This high efficiency is comparable to that achieved in Schwann cell transduction using viral vector AAV6 with a multiplicity of infection of 1000[65], but significantly less cytotoxic effects compared to the 90% cell death associated with viral gene delivery[65]. It is also higher compared to the 10-48% transfection efficiency achieved using other commercially available cationic polymer-based transfection reagents[66,67]. Moreover, transfection using PEI led to sustained but transient gene expression, which is far more desirable for nerve repair than permanent over-expression since supraphysiological protein expression can lead to axonal trapping and other aberrant side-effects seen with viral gene delivery[18,19]. When the transfection efficiency of PEI-pDNA nanoparticles was compared to that of chitosan-pDNA nanoparticles (*Supplementary 1A*), chitosan led to a transfection efficiency of < 5% despite previously being optimized for efficient bone-marrow derived mesenchymal stem cell transfection in successful bone repair applications[26], suggesting that chitosan requires further optimization for Schwann cell transfection. Altering pDNA dose (*Supplementary 2B*) was considered another potential variable to further optimise gene delivery[26,27], however increasing pDNA dose led to increased cytotoxicity likely due to increased PEI concentration used to maintain the N/P ratio constant. Collectively, these findings suggest that the optimal PEI nanoparticle formulation for Schwann cell transfection consists of PEI and a 2 μg dose of pDNA with an N/P ratio of 7.

Having confirmed that PEI-pDNA nanoparticles are suitable the transfection of Schwann cells (S42 cells), we next sought to assess their potential therapeutic effects *in vitro* with genes encoding for therapeutic proteins, *i.e.* neurotrophic factors NGF,

GDNF and the transcription factor c-Jun. Since the nanoparticle were optimized for Schwann cell transfection, we found that Schwann cells could be readily transfected with each of the three genes as expected, leading to 2-fold overexpression of neurotrophic cytokines while also overcoming polymer-associated cytotoxicity by enhancing Schwann cell proliferation. However, we cannot discount the possibility that other cell types in the regenerative microenvironment might also pick up these nanoparticles. For example, sprouting axons might also take up these nanoparticles and transport the particle contents towards the nucleus via retrograde signalling. To test this possibility *in vitro*, in this study we show that DRG neurons can also be transfected, leading to enhanced axonal outgrowth with each of the three genes compared to non-transfected DRG neurons. However, the results indicated that the gene encoding for the transcription factor c-Jun led to 1.45-fold longer axonal outgrowth compared to genes encoding for the neurotrophic cytokines NGF or GDNF, and 2.83-fold longer axonal outgrowth compared to the outgrowth in non-transfected DRGs. These results reflect the potential of c-Jun[48] to upregulate multiple neurotrophic factors including NGF, GDNF and CNTF (as shown in this study), and brain derived neurotrophic factor (BDNF), artemin, and neurotrophin 3 (NT-3) as shown in another study[49]. Furthermore, it has previously been demonstrated that c-Jun also regulates the expression of adhesion molecules such as N-cadherin and neural cell adhesion molecule (NCAM), while governing the morphogenetic processes that transform myelinating Schwann cells to a pro-regenerative phenotype[48] – processes that are highly advantageous for nerve repair. A potential caveat of this approach is that c-Jun is a known proto-oncogene[68] and might lead to potential problems, however a recent study that permanently overexpressed c-Jun in Schwann cells raised no concerns in this regard[49]. Results also suggest that although being optimized for Schwann cell uptake, a gene-activated NGC approach has the potential to lead to axon uptake of nanoparticles[69], which might potentially enhance repair *in vivo*. Corroborating our findings, a recent study[70] has demonstrated the high efficacy of transfecting DRG neuronal cells in the spinal nerve of rats with similar PEI-pDNA nanoparticles, however, carrying their approach required five times the amount of pDNA as in this study – further highlighting the efficiency of our approach. Collectively, these findings suggest that multiple cell types can be targeted using a single gene, while demonstrating that the gene encoding for c-Jun has greater therapeutic potential

than either of the genes encoding specifically for the neurotrophic cytokines, NGF and GDNF.

Loading the PEI-pDNA nanoparticles into the luminal filler of the biphasic NGC developed previously[20] led to the successful development of a gene activated construct, demonstrated by its capacity to transfect Schwann cells (S42 cells) in 3D, exhibiting sustained but transient levels of gene expression over 28 days *in vitro*. A series of gene activated conduits were created by seamlessly incorporating nanoparticles carrying each of the three genes into the luminal filler. Transfection in 3D led to > 2-fold overexpression in Schwann cell neurotrophic cytokines using PEI-pNGF and PEI-pGDNF nanoparticles, and > 3-fold overexpression using PEI-pJUN, again highlighting the greater efficiency of the transcription factor c-Jun *in vitro*. Furthermore, the sustained, paracrine and desired effect of transfected Schwann cells in the gene activated luminal fillers on neurite outgrowth was demonstrated, with the PEI-pJUN-activated luminal filler leading to enhanced neurite outgrowth compared to all other groups. Collectively, this study demonstrates *in vitro* an innovative approach to control the timing, release and level of therapeutic protein production by transfecting Schwann cells to transiently sustain protein production using a gene-activated NGC as the gene delivery platform, while also highlighting the high efficiency of the transcription factor c-Jun compared to NGF and GDNF. The next step in the validation of this approach should involve *in vivo* assessment to determine the level of enhance nerve repair.

5. Conclusion

In this study a gene activated nerve guidance conduit was successfully developed by incorporating non-viral PEI-pDNA nanoparticles capable of efficient Schwann cell transfection *in vitro* with genes encoding for therapeutic NGF, GDNF or c-Jun. This innovative approach may provide an alternative to conduits used as platforms for the delivery neurotrophic factors or genetically modified cells (viral gene therapy), and a potential solution for the unmet clinical need to repair large peripheral nerve injury effectively; however, further *in vivo* studies are required to fully demonstrate this potential.

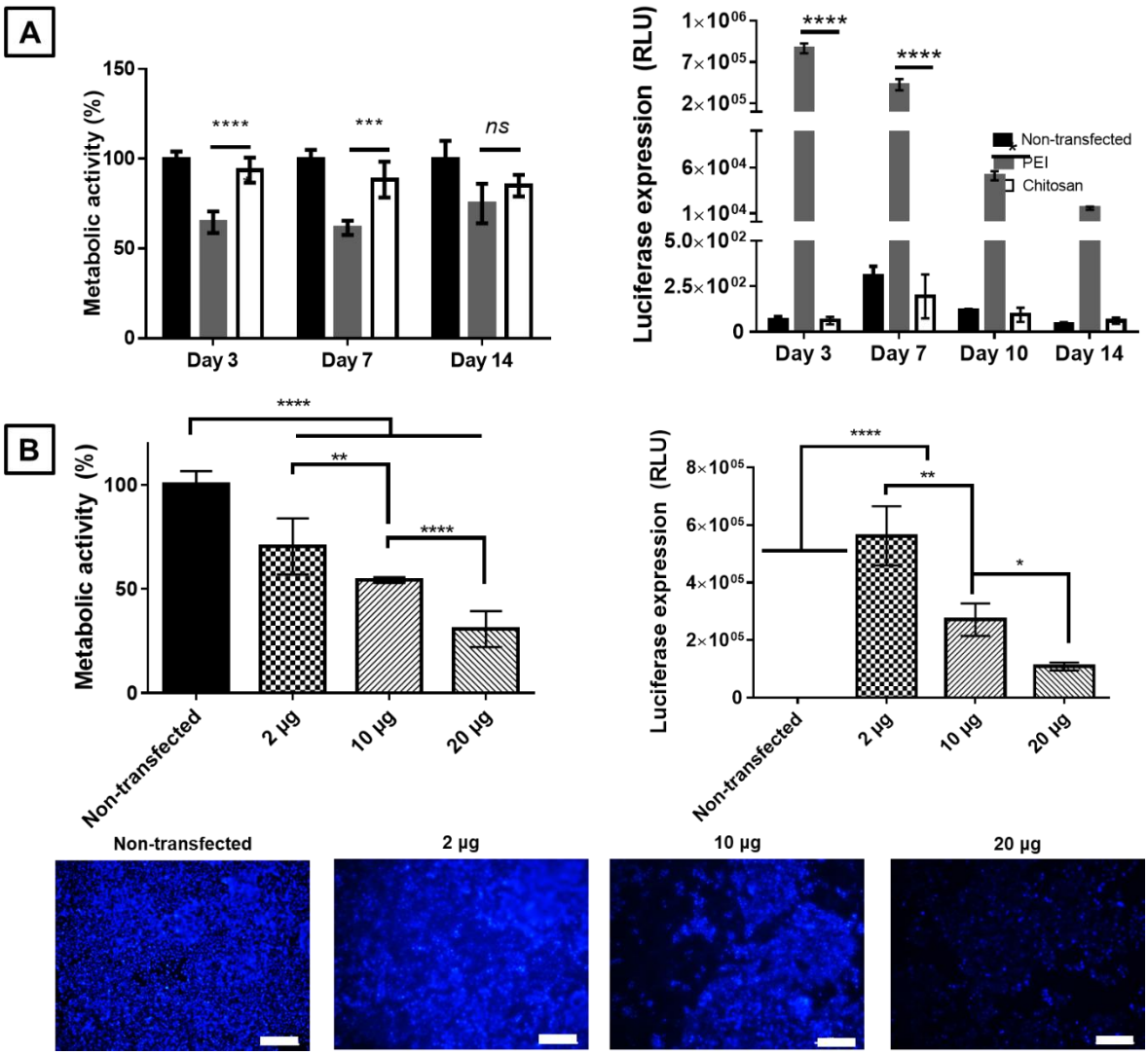

Supplementary 2: Assessment of chitosan-pDNA nanoparticles and increasing pDNA dose

A) Schwann cells were transfected with chitosan-pGLuc nanoparticles (N/P 10, 2 µg pDNA) and their metabolic activity and luciferase expression is reported in comparison to that of cells transfected with PEI-pGLuc (N/P 7, 2 µg pDNA) and non-transfected cells. While chitosan-pDNA nanoparticles rendered significantly lower cytotoxicity than PEI-pDNA nanoparticles after transfection, the latter had far superior transgene expression than the former. Data plotted represents mean ± standard deviation, n = 3. *, *** and **** denote $p<0.05$, $p<0.001$, and $p<0.0001$, respectively, two-way ANOVA. B) Schwann cells were transfected using PEI-pGLuc nanoparticles with increasing pDNA dose (2 µg, 10 µg and 20 µg), and increasing PEI concentration to maintain the N/P ratio (7) constant. The effect of increasing pDNA dose was assessed in terms of metabolic activity and luciferase expression after 7 days in culture, showing stepwise drops in both transgene expression and cell viability in response to increasing pDNA dose, also suggested by cells stained with Hoechst 33258 after 7 days in culture, showing reduced cell densities in response to increasing pDNA dose. Scale bar 200 µm. Data plotted represents mean ± standard deviation, n = 3. *, ** and **** denote $p<0.05$, $p<0.01$, and $p<0.0001$, respectively, one-way ANOVA.

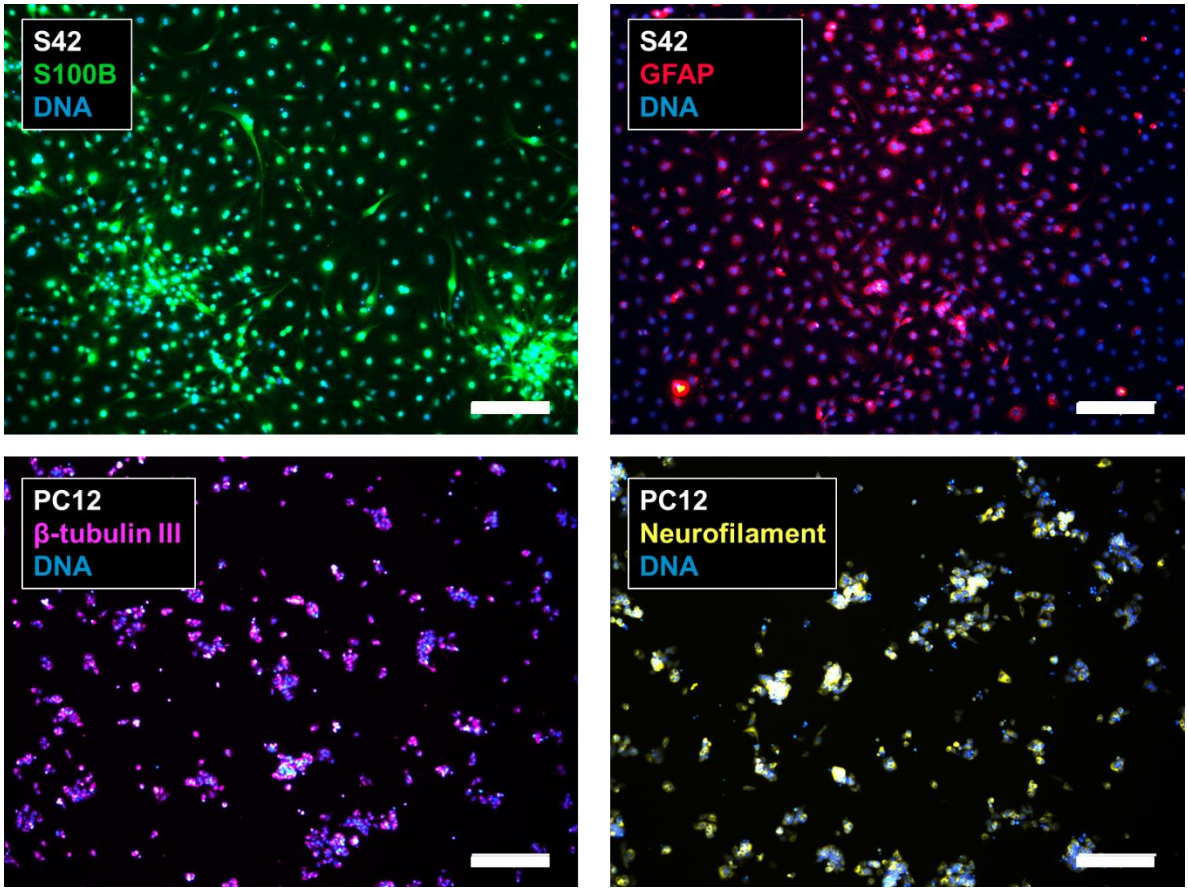

Supplementary 1: Verification of Schwann cell and neuronal phenotypes in S42 and PC12 cell lines

Panels show S42 cells (top) and PC12 cells (bottom) stained using Schwann cell markers S100B and GFAP, and neuronal markers β-tubulin III and neurofilament, and DNA is counterstained using Hoechst 33258. Scale bar 100 µm.

6. Acknowledgements

This study has emanated from research supported from an Irish Research Council Postgraduate Fellowship (Government of Ireland), Grant Number GOIPG/2013/177, and the European Research Council Award Number 239685 (Seventh Framework Programme).

7. References

1. Taylor, C.A., Braza, D., Rice, J.B. and Dillingham, T. 2008. The incidence of peripheral nerve injury in extremity trauma. *American Journal of Physical Medicine & Rehabilitation,* 87(5), pp.381-385.
2. Brattain, K. 2014. Analysis of the peripheral nerve repair market in the united states.
3. Millesi, H. 2007. Bridging defects: Autologous nerve grafts. *How to Improve the Results of Peripheral Nerve Surgery,* pp.37-38.
4. Nectow, A.R., Marra, K.G. and Kaplan, D.L. 2012. Biomaterials for the development of peripheral nerve guidance conduits. *Tissue Engineering.Part B, Reviews,* 18(1), pp.40-50.
5. Lackington, W.A., Ryan, A.J. and O'Brien, F.J. 2017. Advances in nerve guidance conduit-based therapeutics for peripheral nerve repair. *ACS Biomaterials Science & Engineering,* 3(7), pp.1221-1235.
6. de Ruiter, G.C., Malessy, M.J., Yaszemski, M.J., Windebank, A.J. and Spinner, R.J. 2009. Designing ideal conduits for peripheral nerve repair. *Neurosurgical Focus,* 26(2), pp.E5.
7. Farole, A. and Jamal, B.T. 2008. A bioabsorbable collagen nerve cuff (NeuraGen) for repair of lingual and inferior alveolar nerve injuries: A case series. *Journal of Oral and Maxillofacial Surgery : Official Journal of the American Association of Oral and Maxillofacial Surgeons,* 66(10), pp.2058-2062.
8. Poppler, L.H., Ee, X., Schellhardt, L., Hoben, G.M., Pan, D., Hunter, D.A., Yan, Y., Moore, A.M., Snyder-Warwick, A.K., Stewart, S.A., Mackinnon, S.E. and Wood, M.D. 2016. Axonal growth arrests after an increased accumulation of schwann cells expressing senescence markers and stromal cells in acellular nerve allografts. *Tissue Engineering.Part A,* 22(13-14), pp.949-961.
9. Ikeda, M., Uemura, T., Takamatsu, K., Okada, M., Kazuki, K., Tabata, Y., Ikada, Y. and Nakamura, H. 2014. Acceleration of peripheral nerve regeneration using nerve conduits in combination with induced pluripotent stem cell technology and a basic fibroblast growth factor drug delivery system. *Journal of Biomedical Materials Research.Part A,* 102(5), pp.1370-1378.
10. Hu, N., Wu, H., Xue, C., Gong, Y., Wu, J., Xiao, Z., Yang, Y., Ding, F. and Gu, X. 2013. Long-term outcome of the repair of 50 mm long median nerve defects in rhesus monkeys with marrow mesenchymal stem cells-containing, chitosan-based tissue engineered nerve grafts. *Biomaterials,* 34(1), pp.100-111.
11. Cooney, D.S., Wimmers, E.G., Ibrahim, Z., Grahammer, J., Christensen, J.M., Brat, G.A., Wu, L.W., Sarhane, K.A., Lopez, J. and Wallner, C. 2016. Mesenchymal stem cells enhance nerve regeneration in a rat sciatic nerve repair and hindlimb transplant model. *Scientific Reports,* 6pp.31306.
12. Sivak, W.N., White, J.D., Bliley, J.M., Tien, L.W., Liao, H.T., Kaplan, D.L. and Marra, K.G. 2014. Delivery of chondroitinase ABC and glial cell line-derived neurotrophic factor from silk fibroin conduits enhances peripheral nerve regeneration. *Journal of Tissue Engineering and Regenerative Medicine,*
13. Tajdaran, K., Gordon, T., Wood, M.D., Shoichet, M.S. and Borschel, G.H. 2016. A glial cell line-derived neurotrophic factor delivery system enhances nerve regeneration across acellular nerve allografts. *Acta Biomaterialia,* 29pp.62-70.
14. Lee, A.C., Yu, V.M., Lowe, J.B.,3rd, Brenner, M.J., Hunter, D.A., Mackinnon, S.E. and Sakiyama-Elbert, S.E. 2003. Controlled release of nerve growth factor enhances sciatic nerve regeneration. *Experimental Neurology,* 184(1), pp.295-303.
15. Kearney, C.J. and Mooney, D.J. 2013. Macroscale delivery systems for molecular and cellular payloads. *Nature Materials,* 12(11), pp.1004-1017.
16. Zeng, W., Rong, M., Hu, X., Xiao, W., Qi, F., Huang, J. and Luo, Z. 2014.

Incorporation of chitosan microspheres into collagen-chitosan scaffolds for the controlled release of nerve growth factor. *PloS One,* 9(7), pp.e101300.
17. Lin, Y.C., Oh, S.J. and Marra, K.G. 2013. Synergistic lithium chloride and glial cell line-derived neurotrophic factor delivery for peripheral nerve repair in a rodent sciatic nerve injury model. *Plastic and Reconstructive Surgery,* 132(2), pp.251e-262e.
18. Eggers, R., de Winter, F., Hoyng, S.A., Roet, K.C., Ehlert, E.M., Malessy, M.J., Verhaagen, J. and Tannemaat, M.R. 2013. Lentiviral vector-mediated gradients of GDNF in the injured peripheral nerve: Effects on nerve coil formation, schwann cell maturation and myelination. *PloS One,* 8(8), pp.e71076.
19. Santosa, K.B., Jesuraj, N.J., Viader, A., MacEwan, M., Newton, P., Hunter, D.A., Mackinnon, S.E. and Johnson, P.J. 2013. Nerve allografts supplemented with schwann cells overexpressing glial-cell-line-derived neurotrophic factor. *Muscle & Nerve,* 47(2), pp.213-223.
20. Ryan, A.J., Lackington, W.A., Hibbitts, A.J., Matheson, A., Alekseeva, T., Stejskalova, A., Roche, P. and O'Brien, F.J. 2017. A physicochemically optimized and neuroconductive biphasic nerve guidance conduit for peripheral nerve repair. *Advanced Healthcare Materials,*
21. Roche, P., Alekseeva, T., Widaa, A., Ryan, A., Matsiko, A., Walsh, M., Duffy, G. and O'Brien, F.J. 2017. Olfactory derived stem cells delivered in a bi-phasic conduit promote peripheral nerve repair in vivo *STEM CELLS Translational Medicine,* 10.1002/sctm.16-0420
22. Quinlan, E., López- Noriega, A., Thompson, E.M., Hibbitts, A., Cryan, S.A. and O'Brien, F.J. 2017. Controlled release of vascular endothelial growth factor from spray- dried alginate microparticles in collagen–hydroxyapatite scaffolds for promoting vascularization and bone repair. *Journal of Tissue Engineering and Regenerative Medicine,* 11(4), pp.1097-1109.
23. Quinlan, E., Thompson, E.M., Matsiko, A., O'brien, F.J. and López-Noriega, A. 2015. Long-term controlled delivery of rhBMP-2 from collagen–hydroxyapatite scaffolds for superior bone tissue regeneration. *Journal of Controlled Release,* 207pp.112-119.
24. Tria, M.A., Fusco, M., Vantini, G. and Mariot, R. 1994. Pharmacokinetics of nerve growth factor (NGF) following different routes of administration to adult rats. *Experimental Neurology,* 127(2), pp.178-183.
25. Bryan, D.J., Litchfield, C.R., Manchio, J.V., Logvinenko, T., Holway, A.H., Austin, J., Summerhayes, I.C. and Rieger-Christ, K.M. 2012. Spatiotemporal expression profiling of proteins in rat sciatic nerve regeneration using reverse phase protein arrays. *Proteome Science,* 10(1), pp.9-5956-10-9.
26. Raftery, R.M., Tierney, E.G., Curtin, C.M., Cryan, S.A. and O'Brien, F.J. 2015. Development of a gene-activated scaffold platform for tissue engineering applications using chitosan-pDNA nanoparticles on collagen-based scaffolds. *Journal of Controlled Release : Official Journal of the Controlled Release Society,* 210pp.84-94.
27. Tierney, E.G., Duffy, G.P., Hibbitts, A.J., Cryan, S.A. and O'Brien, F.J. 2012. The development of non-viral gene-activated matrices for bone regeneration using polyethyleneimine (PEI) and collagen-based scaffolds. *Journal of Controlled Release : Official Journal of the Controlled Release Society,* 158(2), pp.304-311.
28. Mencia Castano, I., Curtin, C.M., Duffy, G.P. and O'Brien, F.J. 2016. Next generation bone tissue engineering: Non-viral miR-133a inhibition using collagen-nanohydroxyapatite scaffolds rapidly enhances osteogenesis. *Scientific Reports,* 6pp.27941.
29. Raftery, R.M., Mencia Castano, I., Chen, G., Cavanagh, B., Quinn, B., Curtin, C.M., Cryan, S.A. and O'Brien, F.J. 2017. Translating the role of osteogenic-angiogenic coupling in bone formation: Highly efficient chitosan-pDNA activated scaffolds can

accelerate bone regeneration in critical-sized bone defects. *Biomaterials,* 149pp.116-127.
30. Curtin, C.M., Tierney, E.G., McSorley, K., Cryan, S., Duffy, G.P. and O'brien, F.J. 2015. Combinatorial gene therapy accelerates bone regeneration: Non-viral dual delivery of VEGF and BMP2 in a collagen- nanohydroxyapatite scaffold. *Advanced Healthcare Materials,* 4(2), pp.223-227.
31. Hoyng, S.A., de Winter, F., Tannemaat, M.R., Blits, B., Malessy, M.J. and Verhaagen, J. 2015. Gene therapy and peripheral nerve repair: A perspective. *Frontiers in Molecular Neuroscience,* 8pp.32.
32. Raftery, R.M., Walsh, D.P., Castaño, I.M., Heise, A., Duffy, G.P., Cryan, S. and O'Brien, F.J. 2016. Delivering Nucleic- Acid based nanomedicines on biomaterial scaffolds for orthopedic tissue repair: Challenges, progress and future perspectives. *Advanced Materials,* 28(27), pp.5447-5469.
33. Mason, M.R., Tannemaat, M.R., Malessy, M.J. and Verhaagen, J. 2011. Gene therapy for the peripheral nervous system: A strategy to repair the injured nerve? *Current Gene Therapy,* 11(2), pp.75-89.
34. Tannemaat, M.R., Verhaagen, J. and Malessy, M. 2008a. The application of viral vectors to enhance regeneration after peripheral nerve repair. *Neurological Research,* 30(10), pp.1039-1046.
35. Fischer, D., Bieber, T., Li, Y., Elsasser, H.P. and Kissel, T. 1999. A novel non-viral vector for DNA delivery based on low molecular weight, branched polyethylenimine: Effect of molecular weight on transfection efficiency and cytotoxicity. *Pharmaceutical Research,* 16(8), pp.1273-1279.
36. Ramamoorth, M. and Narvekar, A. 2015. Non viral vectors in gene therapy-an overview. *Journal of Clinical and Diagnostic Research : JCDR,* 9(1), pp.GE01-6.
37. Boussif, O., Lezoualc'h, F., Zanta, M.A., Mergny, M.D., Scherman, D., Demeneix, B. and Behr, J.P. 1995. A versatile vector for gene and oligonucleotide transfer into cells in culture and in vivo: Polyethylenimine. *Proceedings of the National Academy of Sciences of the United States of America,* 92(16), pp.7297-7301.
38. Kafil, V. and Omidi, Y. 2011. Cytotoxic impacts of linear and branched polyethylenimine nanostructures in a431 cells. *BioImpacts : BI,* 1(1), pp.23-30.
39. Florea, B.I., Meaney, C., Junginger, H.E. and Borchard, G. 2002. Transfection efficiency and toxicity of polyethylenimine in differentiated calu-3 and nondifferentiated COS-1 cell cultures. *AAPS pharmSci,* 4(3), pp.E12.
40. McMahon, S.B., Bennett, D.L., Priestley, J.V. and Shelton, D.L. 1995. The biological effects of endogenous nerve growth factor on adult sensory neurons revealed by a trkA-IgG fusion molecule. *Nature Medicine,* 1(8), pp.774-780.
41. Hoke, A., Ho, T., Crawford, T.O., LeBel, C., Hilt, D. and Griffin, J.W. 2003. Glial cell line-derived neurotrophic factor alters axon schwann cell units and promotes myelination in unmyelinated nerve fibers. *The Journal of Neuroscience : The Official Journal of the Society for Neuroscience,* 23(2), pp.561-567.
42. Yu, T., Scully, S., Yu, Y., Fox, G.M., Jing, S. and Zhou, R. 1998. Expression of GDNF family receptor components during development: Implications in the mechanisms of interaction. *The Journal of Neuroscience : The Official Journal of the Society for Neuroscience,* 18(12), pp.4684-4696.
43. Rich, K.M., Luszczynski, J.R., Osborne, P.A. and Johnson, E.M.,Jr. 1987. Nerve growth factor protects adult sensory neurons from cell death and atrophy caused by nerve injury. *Journal of Neurocytology,* 16(2), pp.261-268.
44. Henderson, C.E., Phillips, H.S., Pollock, R.A., Davies, A.M., Lemeulle, C., Armanini, M., Simmons, L., Moffet, B., Vandlen, R.A., Simpson LC corrected to Simmons,L., Koliatsos, V.E. and Rosenthal, A. 1994. GDNF: A potent survival factor for motoneurons present in peripheral nerve and muscle. *Science (New York, N.Y.),* 266(5187), pp.1062-1064.

45. Hu, X., Cai, J., Yang, J. and Smith, G.M. 2010. Sensory axon targeting is increased by NGF gene therapy within the lesioned adult femoral nerve. *Experimental Neurology,* 223(1), pp.153-165.
46. Tannemaat, M.R., Verhaagen, J. and Malessy, M. 2008b. The application of viral vectors to enhance regeneration after peripheral nerve repair. *Neurological Research,* 30(10), pp.1039-1046.
47. Catrina, S., Gander, B. and Madduri, S. 2013. Nerve conduit scaffolds for discrete delivery of two neurotrophic factors. *European Journal of Pharmaceutics and Biopharmaceutics : Official Journal of Arbeitsgemeinschaft Fur Pharmazeutische Verfahrenstechnik E.V,* 85(1), pp.139-142.
48. Arthur-Farraj, P.J., Latouche, M., Wilton, D.K., Quintes, S., Chabrol, E., Banerjee, A., Woodhoo, A., Jenkins, B., Rahman, M., Turmaine, M., Wicher, G.K., Mitter, R., Greensmith, L., Behrens, A., Raivich, G., Mirsky, R. and Jessen, K.R. 2012. C-jun reprograms schwann cells of injured nerves to generate a repair cell essential for regeneration. *Neuron,* 75(4), pp.633-647.
49. Huang, L., Quan, X., Liu, Z., Ma, T., Wu, Y., Ge, J., Zhu, S., Yang, Y., Liu, L., Sun, Z., Huang, J. and Luo, Z. 2015. C-jun gene-modified schwann cells: Upregulating multiple neurotrophic factors and promoting neurite outgrowth. *Tissue Engineering.Part A,* 21(7-8), pp.1409-1421.
50. Yang, Y. and Burkhard, P. 2012. Encapsulation of gold nanoparticles into self-assembling protein nanoparticles. *Journal of Nanobiotechnology,* 10pp.42-3155-10-42.
51. Schindelin, J., Arganda-Carreras, I., Frise, E., Kaynig, V., Longair, M., Pietzsch, T., Preibisch, S., Rueden, C., Saalfeld, S., Schmid, B., Tinevez, J.Y., White, D.J., Hartenstein, V., Eliceiri, K., Tomancak, P. and Cardona, A. 2012. Fiji: An open-source platform for biological-image analysis. *Nature Methods,* 9(7), pp.676-682.
52. Toda, K., Small, J.A., Goda, S. and Quarles, R.H. 1994. Biochemical and cellular properties of three immortalized schwann cell lines expressing different levels of the myelin-associated glycoprotein. *Journal of Neurochemistry,* 63(5), pp.1646-1657.
53. Greene, L.A. and Tischler, A.S. 1976. Establishment of a noradrenergic clonal line of rat adrenal pheochromocytoma cells which respond to nerve growth factor. *Proceedings of the National Academy of Sciences of the United States of America,* 73(7), pp.2424-2428.
54. Paivalainen, S., Nissinen, M., Honkanen, H., Lahti, O., Kangas, S.M., Peltonen, J., Peltonen, S. and Heape, A.M. 2008. Myelination in mouse dorsal root ganglion/schwann cell cocultures. *Molecular and Cellular Neurosciences,* 37(3), pp.568-578.
55. Longair, M.H., Baker, D.A. and Armstrong, J.D. 2011. Simple neurite tracer: Open source software for reconstruction, visualization and analysis of neuronal processes. *Bioinformatics (Oxford, England),* 27(17), pp.2453-2454.
56. Hamill, O.P., Marty, A., Neher, E., Sakmann, B. and Sigworth, F.J. 1981. Improved patch-clamp techniques for high-resolution current recording from cells and cell-free membrane patches. *Pflugers Archiv : European Journal of Physiology,* 391(2), pp.85-100.
57. Russell, S., Bennett, J., Wellman, J.A., Chung, D.C., Yu, Z., Tillman, A., Wittes, J., Pappas, J., Elci, O. and McCague, S. 2017. Efficacy and safety of voretigene neparvovec (AAV2-hRPE65v2) in patients with RPE65-mediated inherited retinal dystrophy: A randomised, controlled, open-label, phase 3 trial. *The Lancet,* 390(10097), pp.849-860.
58. Mendell, J.R., Al-Zaidy, S., Shell, R., Arnold, W.D., Rodino-Klapac, L.R., Prior, T.W., Lowes, L., Alfano, L., Berry, K. and Church, K. 2017. Single-dose gene-replacement therapy for spinal muscular atrophy. *New England Journal of Medicine,* 377(18), pp.1713-1722.

59. Hirsch, T., Rothoeft, T., Teig, N., Bauer, J.W., Pellegrini, G., De Rosa, L., Scaglione, D., Reichelt, J., Klausegger, A., Kneisz, D., Romano, O., Secone Seconetti, A., Contin, R., Enzo, E., Jurman, I., Carulli, S., Jacobsen, F., Luecke, T., Lehnhardt, M., Fischer, M., Kueckelhaus, M., Quaglino, D., Morgante, M., Bicciato, S., Bondanza, S. and De Luca, M. 2017. Regeneration of the entire human epidermis using transgenic stem cells. *Nature,*
60. Goula, D., Remy, J.S., Erbacher, P., Wasowicz, M., Levi, G., Abdallah, B. and Demeneix, B.A. 1998. Size, diffusibility and transfection performance of linear PEI/DNA complexes in the mouse central nervous system. *Gene Therapy,* 5(5), pp.712-717.
61. Rudolph, C., Muller, R.H. and Rosenecker, J. 2002. Jet nebulization of PEI/DNA polyplexes: Physical stability and in vitro gene delivery efficiency. *The Journal of Gene Medicine,* 4(1), pp.66-74.
62. Poon, G.M. and Gariepy, J. 2007. Cell-surface proteoglycans as molecular portals for cationic peptide and polymer entry into cells. *Biochemical Society Transactions,* 35(Pt 4), pp.788-793.
63. Evans, C.W., Fitzgerald, M., Clemons, T.D., House, M.J., Padman, B.S., Shaw, J.A., Saunders, M., Harvey, A.R., Zdyrko, B., Luzinov, I., Silva, G.A., Dunlop, S.A. and Iyer, K.S. 2011. Multimodal analysis of PEI-mediated endocytosis of nanoparticles in neural cells. *ACS Nano,* 5(11), pp.8640-8648.
64. Moret, I., Esteban Peris, J., Guillem, V.M., Benet, M., Revert, F., Dasi, F., Crespo, A. and Alino, S.F. 2001. Stability of PEI-DNA and DOTAP-DNA complexes: Effect of alkaline pH, heparin and serum. *Journal of Controlled Release : Official Journal of the Controlled Release Society,* 76(1-2), pp.169-181.
65. Hoyng, S.A., De Winter, F., Gnavi, S., van Egmond, L., Attwell, C.L., Tannemaat, M.R., Verhaagen, J. and Malessy, M.J. 2015. Gene delivery to rat and human schwann cells and nerve segments: A comparison of AAV 1-9 and lentiviral vectors. *Gene Therapy,* 22(10), pp.767-780.
66. Haastert, K., Mauritz, C., Chaturvedi, S. and Grothe, C. 2007. Human and rat adult schwann cell cultures: Fast and efficient enrichment and highly effective non-viral transfection protocol. *Nature Protocols,* 2(1), pp.99-104.
67. Kraus, A., Tager, J., Kohler, K., Haerle, M., Werdin, F., Schaller, H.E. and Sinis, N. 2010. Non-viral genetic transfection of rat schwann cells with FuGENE HD(c) lipofection and AMAXA(c) nucleofection is feasible but impairs cell viability. *Neuron Glia Biology,* 6(4), pp.225-230.
68. Mathas, S., Hinz, M., Anagnostopoulos, I., Krappmann, D., Lietz, A., Jundt, F., Bommert, K., Mechta-Grigoriou, F., Stein, H., Dorken, B. and Scheidereit, C. 2002. Aberrantly expressed c-jun and JunB are a hallmark of hodgkin lymphoma cells, stimulate proliferation and synergize with NF-kappa B. *The EMBO Journal,* 21(15), pp.4104-4113.
69. Raper, J. and Mason, C. 2010. Cellular strategies of axonal pathfinding. *Cold Spring Harbor Perspectives in Biology,* 2(9), pp.a001933.
70. Chang, M.F., Hsieh, J.H., Chiang, H., Kan, H.W., Huang, C.M., Chellis, L., Lin, B.S., Miaw, S.C., Pan, C.L., Chao, C.C. and Hsieh, S.T. 2016. Effective gene expression in the rat dorsal root ganglia with a non-viral vector delivered via spinal nerve injection. *Scientific Reports,* 6pp.35612.